LICK OBSERVATORY

TECHNICAL REPORT

78

DEIMOS Collimator and Slit Mask Surface Design and End-to-End System Performance

Brian M. Sutin
Lick Observatory
University of California
Santa Cruz, California
March 31, 1995

UNIVERSITY OF CALIFORNIA SANTA CRUZ

CONTENTS

§1 INTRODUCTION

This technical report gives design parameters for the DEIMOS collimating mirror and the shape of the slit mask surface. End-to-end performance characteristics with and without the adopted Epps camera design Run No. 3761 (03/02/95) are included.

Several different effects are compared. The first is the effect of pulling DEIMOS away from the nominal telescope focus by 3.0 inches. The second is the choice of either a spherical or cylindrical shape for the slit mask surface. The third is the added aberrations solely due to the adopted Epps (3761) camera design, as opposed to a perfect 15.0-inch camera.

§2 ASSUMPTIONS AND CONVENTIONS

The following assumptions and conventions were used for all calculations. Inches are used in the text throughout; however, the plots often display values in microns, which is an unavoidable result of the software. Object field positions are given in arcmin, and image spot sizes are given in arcsec.

The Keck telescope primary was assumed to be a circular monolithic mirror. The input aperture was set to be at the primary, with an inner diameter of 104.0 inches, corresponding to the blockage of the secondary mirror shroud, and an outer diameter of 402.0 inches, which is a reasonable approximation to the serrated outer edge of the segmented primary. Using these inner and outer diameters, the rms spot sizes for a few cases were checked against a model of the true aperture, and were found to be in reasonable agreement. Except for the vignetting which takes place at the camera mouth of the Epps (3761) camera design, no other vignetting occurs anywhere in the design or modeling.

The secondary mirror surface was assumed to have the as-built Keck I parameters, with a radius of curvature of -186.53685 inches and a conic constant of -1.64361. The secondary

mirror was allowed to piston for focus.

The collimator has an input design value for the radius of curvature of -173.0 inches, or a focal length of 86.5 inches, set by the beam size and final image scale. All optimizations in which the distance from the collimator to the focal surface of the telescope was allowed to vary gave a value within 0.1 inches of the collimator focal length, 86.5 inches, so the collimator distance was set to this value. Allowing this distance to vary results in defocussing the images near the telescope axis while slightly improving the outer images; the trade off is extremely poor. The final beam was then imaged by either a perfect, 15.0-inch paraxial camera, or the Epps (3761) camera to give the final spot diagrams and rms spot diameters. A perfect paraxial camera is a camera with an entrance pupil of infinite diameter and no aberrations. All spot diagrams in this report are imaged with the perfect camera unless explicitly noted as imaged by the Epps (3761) camera.

The free parameters remaining in the system are the conic constant of the collimator mirror, the position of the secondary focus, and the shape and position of the slit mask surface for spectroscopy. Collimator surface shape terms of higher order than the $A_2 = -e^2$ conic constant were found to have a negligible effect on the system. Since the DEIMOS spectrograph is likely to be pulled away from the nominal focal surface of the telescope by about 3.0 inches in order to accommodate the slit mask handling mechanism, the cases with and without pullback are compared.

For the design of the collimator and slit mask surface, 9 points were chosen in the field of the telescope to represent the overall quality of the DEIMOS field of view. Figure 2.1 shows these field positions. The outer circle corresponds to the 10.0-arcmin maximum field of view. The lower, upper, and outer boundaries corresponding to approximately 8 arcmin are the outer edges of the chip. The inner edges correspond to the area vignetted by the tent mirrors. The area to the right of point 9 in the diagram is also vignetted by the camera body, but this vignetting is not shown. In most cases, point 2 corresponds to the end of a typical slit, while point 3 corresponds to the worst case for imaging. Table 2.1 shows the X

and Y field positions and angular radii of each point from the center of the field of both the telescope and the camera.

Table 2.1

Spot Number	Telescope X arcmin	Telescope Y arcmin	Telescope Radius arcmin	Camera X arcmin	Camera Y arcmin	Camera Radius arcmin
1	3.00	8.00	8.54	-2.00	8.00	8.25
2	5.00	8.00	9.43	0.00	8.00	8.00
3	7.00	7.14	10.00	2.00	7.14	7.41
4	3.00	4.00	5.00	-2.00	4.00	4.47
5	5.00	4.00	6.40	0.00	4.00	4.00
6	7.00	4.00	8.06	2.00	4.00	4.47
7	3.00	0.00	3.00	-2.00	0.00	2.00
8	5.00	0.00	5.00	0.00	0.00	0.00
9	7.00	0.00	7.00	2.00	0.00	2.00

§3 COLLIMATOR

Figure 3.1 shows the spots at the nominal focal surface of the telescope, before being imaged by the collimator and camera. The field curvature radius used is -84.7 inches. The spot size is due to astigmatism, and the slight darkening of the inner edge of the spot is from to the small amount of coma introduced by the imperfectly matched conic constant of the Keck I secondary mirror. Since the collimator displays negative coma, this coma effect probably improves rather than degrades the final imaging quality.

Figures 3.2, 3.3, and 3.4 show the images made by a perfect camera resulting from a collimator with a conic constant of -0.80, -0.75, and -070, respectively. The morphology of these spots are interesting as a sequence. For a value of -0.80, the astigmatism of the telescope dominates, but the negative coma is beginning to fold the spot over itself. For a value of -0.75, the negative coma has folded the spot in half, such that the rms spot diameter is approximately the same as for the telescope alone. For a value of -0.70, the negative coma is dominant, and the rms spot size grows again. The actual minimum rms spot diameter at the edge of the field takes place at -0.7511, which gives the same rms spot diameter as -0.75 to within 4 decimal places. This value also is very near the minimum

geometric spot size, and clearly gives the most compact morphology. A collimator conic constant of -0.75 is therefore adopted for all remaining calculations. Table 3.1 shows a comparison of the rms spot size with respect to the conic parameter.

Table 3.1

Spot Number	Telescope Focus Figure 3.1 arcsec	Collimator Reimaged $A_2 = -0.80$ Figure 3.2 arcsec	$A_2 = -0.75$ Figure 3.3 arcsec	$A_2 = -0.70$ Figure 3.4 arcsec
1	0.25	0.29	0.28	0.29
2	0.31	0.34	0.32	0.34
3	0.34	0.37	0.36	0.37
4	0.09	0.14	0.14	0.14
5	0.14	0.19	0.19	0.19
6	0.22	0.27	0.26	0.26
7	0.03	0.08	0.08	0.07
8	0.09	0.14	0.14	0.14
9	0.17	0.22	0.21	0.21

If the DEIMOS spectrograph is now pulled away from the focus of the telescope by 3.0 inches, and the telescope is refocussed by exactly 3.0 inches to compensate, then the collimator conic constant which gives the minimum rms spot size at the edge of the field has the same -0.75 value as with no pullback. Figure 3.5 shows the images in the new, pulled-back focal surface, and Figure 3.6 shows the these spots imaged by a perfect camera through the collimator. Table 3.4 compares the nominal and 3.0-inch pullback cases.

Table 3.2

Spot Number	Telescope Focal Surface Nominal Figure 3.1 arcsec	3" Pullback Figure 3.3 arcsec	Collimator Reimaged Nominal Figure 3.5 arcsec	3" Pullback Figure 3.6 arcsec
1	0.25	0.25	0.28	0.29
2	0.31	0.31	0.32	0.34
3	0.34	0.35	0.36	0.37
4	0.09	0.09	0.14	0.15
5	0.14	0.15	0.19	0.20
6	0.22	0.23	0.26	0.27
7	0.03	0.05	0.08	0.09
8	0.09	0.09	0.14	0.15
9	0.17	0.17	0.21	0.22

Figure 3.7 shows the through-focus spots for the 3.0-inch pullback case. If the comatic tails on the spots are objectionable, then Figure 3.7 demonstrates that the camera may be slightly defocussed to eliminate these tails.

The next 3 Figures show the image degradation caused by introducing the 'real' Epps (3761) camera in direct imaging mode. While all the previous Figures have been drawn with 0.5-arcsec boxes, these 3 Figures are drawn with 1.0-arcsec boxes, due to the larger spread in the geometric spot sizes. Figure 3.8 has the spots which result from a perfect paraxial camera, while Figure 3.9 has the Epps (3761) camera operating in photometric 'V' band, and Figure 3.10 has the Epps (3761) camera operating in photometric 'B' band. Here 'V' band consists of equally weighted wavelengths of (0.505, 0.520, 0.530, 0.540, 0.550, 0.560, 0.580, 0.605, and 0.640) microns, and 'B' band consists of equally weighted wavelengths of (0.390, 0.400, 0.410, 0.420, 0.430, 0.440, 0.460, 0.480, and 0.500) microns. Table 3.3 compares the rms spot sizes.

Table 3.3

Spot Number	Perfect Camera Monochromatic Figure 3.8 arcsec	Epps (3761) Camera 'V' Band Figure 3.9 arcsec	Epps (3761) Camera 'B' Band Figure 3.10 arcsec
1	0.29	0.30	0.38
2	0.34	0.34	0.41
3	0.37	0.38	0.42
4	0.15	0.20	0.21
5	0.20	0.24	0.25
6	0.27	0.31	0.31
7	0.09	0.15	0.12
8	0.15	0.21	0.17
9	0.22	0.27	0.25

In summation, the major contribution to the rms spot diameters when using DEIMOS in direct imaging mode is from the telescope. For the worst case, at the edge of the field in the 'B' band, the telescope has an rms spot diameter of 0.34 arcsec and the complete system with the Epps (3761) camera has a 0.42 arcsec spotsize. If the aberrations add in quadrature (which they may not), then DEIMOS contributes only 0.24 rms to the rms image diameter, compared to 0.34 rms from the telescope.

§4 SLIT MASK SURFACE

In order to calculate the best slit mask surface shape, each slit was assumed to be a perfect point source which is illuminated directly by the entrance pupil of the telescope. The physical assumption is that all the aberrations of the telescope are lost after passage through a slit. Two criteria are important for evaluating the effect of the collimator on the quality of DEIMOS as a spectrograph: how well the slits are illuminated by the telescope and the final images of the point-slits. If the slit mask is assumed to correspond to a spherical surface with the nominal focal surface curvature, then the slit mask illumination patterns at the nominal focus and with a 3.0-inch pullback have already been displayed in Figures 3.1 and 3.3. Since the effect at the focal surface due to the 3.0-inch pullback, shown in Table 3.2, has a negligible effect on the slit illumination, the 3.0-inch pullback is assumed from this point onwards. The pullback has no effect on the spectrograph after the light passes through the slit.

When the collimator is imaging the point-slits, the best focal surface curvature does not coincide with the telescope focal surface curvature and the best curvature depends on the collimator conic constant. If the value of $A_2 = -0.75$ is chosen for imaging, then the focal surface curvature giving the best rms spotsize at the edge of the telescope field is -81.93 inches. The resulting slit illumination by the telescope is shown in Figure 4.1, and the resulting slit images made by a perfect camera are shown in Figure 4.2. All spot diagrams in this Section have 0.5-arcsec boxes.

Because of the difficulty in making slit masks which are spherical, a slit mask surface which is cylindrical and roughly tangent to the focal surface is much easier to engineer, allowing flat slit masks which are wrapped into a cylinder. By equally weighting the 9 points chosen over the field and optimizing for best rms spot size, the best cylinder has a curvature of -81.57 inches in the y direction. The cylinder is tilted at -6.0 degrees from the collimator axis, and intersects the optical axis 0.4 inches closer to the collimator than the

nominal distance of 86.5 inches. The slit mask surface could be moved closer to the collimator (or refocus), which would improve the images along a slit at the center of the camera field at the expense of the outboard slitlets. Figure 4.3 shows the telescope illumination pattern for the cylindrical surface, and Figure 4.4 shows the resulting slit images. Table 4.1 compares a spherical surface to a cylindrical surface.

Table 4.1

Spot Number	Illumination		Spot Image	
	Spherical Figure 4.1 arcsec	Cylindrical Figure 4.3 arcsec	Spherical Figure 4.2 arcsec	Cylindrical Figure 4.4 arcsec
1	0.26	0.26	0.22	0.23
2	0.32	0.35	0.25	0.26
3	0.36	0.35	0.27	0.27
4	0.10	0.09	0.12	0.13
5	0.15	0.19	0.16	0.18
6	0.23	0.23	0.21	0.21
7	0.05	0.06	0.07	0.08
8	0.10	0.14	0.12	0.15
9	0.18	0.17	0.18	0.18

§5 SPECTROSCOPY

This section shows the performance of DEIMOS in spectrograph mode. Because an exhaustive exploration of the large number of possible gratings and tilts would be unreasonable, only the worst case is explored. the 1200-line/mm grating centered at 0.8000 microns was chosen as the most demanding case for which the camera was specifically designed. Since the camera aberrations cause a larger halo of stray light in this extreme mode of operation, the box sizes on the Figures are 2.0-arcsec across. One slit across the entire field was chosen, centered at 5.0 minutes off the axis of the telescope, corresponding to the center of the camera at 0.8000 microns, and spanning the entire width of the CCD chip mosaic. Four field positions were studied, corresponding to 0%, 80%, 90%, and 100% of the maximum slit length. The slit length from center to end is 8.15 arcmin. Three wavelengths were studied, 0.6960, 0.8000, and 0.882 microns, which were chosen to put the

light from the end of the slit at the center and the very edges of the camera's designed field of view.

Figure 5.1 shows the images of point sources at the focal surface of the collimator, imaged by a perfect camera. The images show are for 0.8000 microns, but the spot shapes do not depend of wavelength with a perfect camera. Figures 5.2, 5.3, and 5.4 show the spots from point sources for 0.6960, 0.8000, and 0.8820 microns, when imaged by a real camera. The camera causes wings to emerge from the spots, mainly in the dispersion direction, which rotate with wavelength. Table 5.1 compares the rms spot diameters for the different wavelengths.

Table 5.1

Slit Position	Perfect Camera Figure 5.1 arcsec	Epps (3761) Camera 0.6960μ Figure 5.2 arcsec	0.8000μ Figure 5.3 arcsec	0.8820μ Figure 5.4 arcsec
0%	0.09	0.17	0.17	0.19
80%	0.18	0.20	0.23	0.26
90%	0.19	0.22	0.27	0.31
100%	0.21	0.25	0.34	0.37

The remaining Figures were all generated by replacing the previous point light source on the slit mask surface with a uniformly illuminated disk of light 0.5 arcsec in diameter. All of these Figures are of the light from the 100% point, at the very end of the slit. Figure 5.5 shows the spot images by a perfect camera. The light is almost completely contained within an ellipse with a width in the dispersion direction of 4 pixels, and a width in the slit direction of 8 pixels. Figures 5.6, 5.7, and 5.8 show the equivalent spots for the Epps (3761) camera at the 3 previously mentioned wavelengths. In Figures 5.9, 5.10, 5.11, and 5.12, a disk with a width in the dispersion direction of 4 pixels and a width in the slit direction of 6 pixels was placed over the center of the spot, leaving mostly the tails. Table 5.2 compares the amount of light in the tails for various wavelengths.

Table 5.2	
Wavelength microns	Light in Tail Percent
Perfect Camera	3.3
0.6960	7.5
0.8000	14.1
0.8820	15.2

§6 CONCLUSIONS

The following conclusions may be drawn from this report:

1) Pulling the DEIMOS spectrograph away from the nominal focus of the Keck telescope by 3.0 inches causes only a small degradation in performance, on the order of 5% or less in the rms spot diameter when imaging.

2) Using a cylindrical rather than spherical shape for the slit mask surface also causes only a small degradation in performance of about the same magnitude as the 3.0-inch pullback.

3) The end-to-end system performance of DEIMOS with the Epps (3761) camera, for both imaging and spectroscopy, gives at worst an 0.4 arcsec rms diameter instrument.

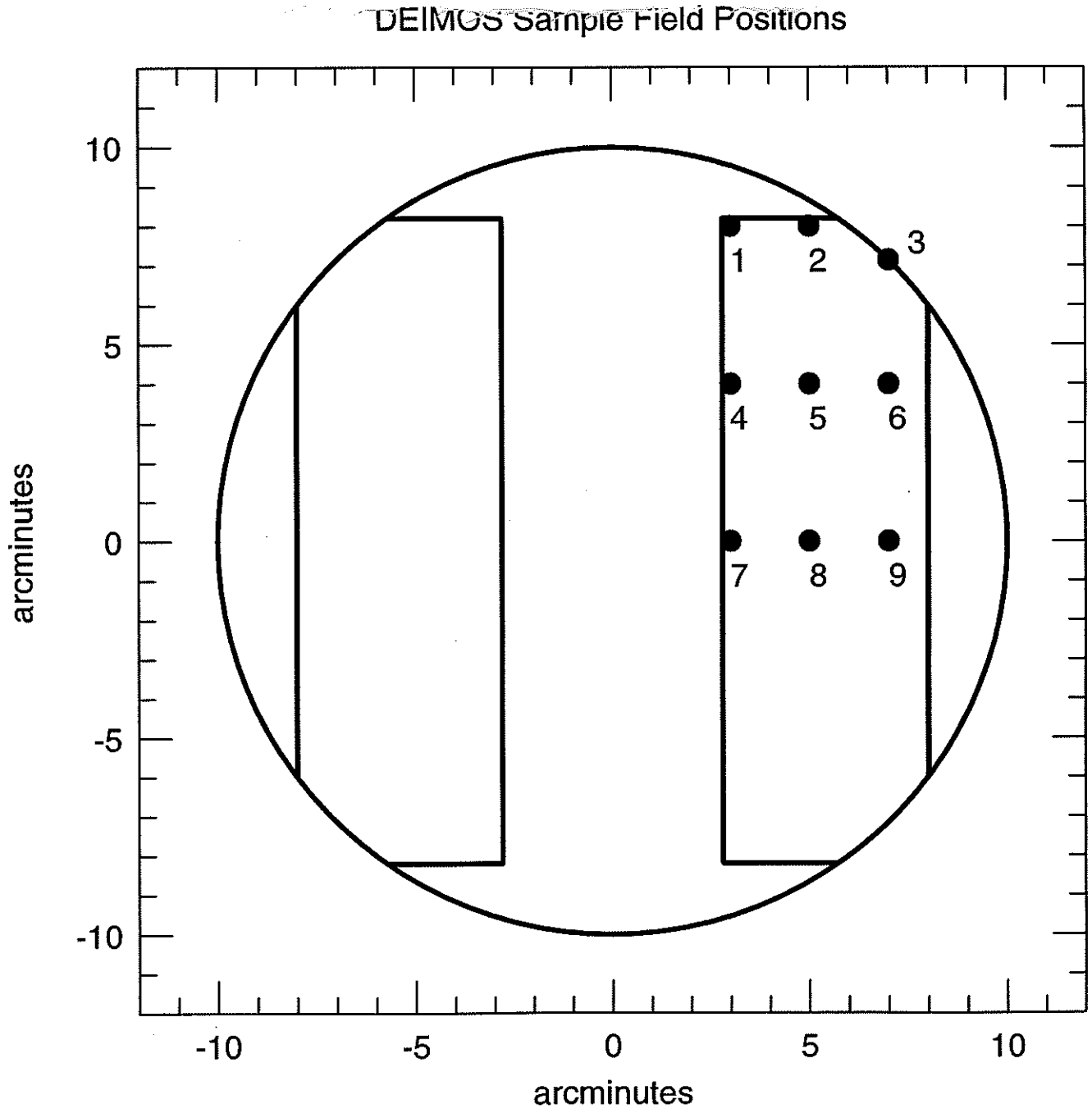
DEIMOS Sample Field Positions
10
5
0
-5
-10
arcminutes
-10
-5
0
5
10
arcminutes
1
2
3
4
5
6
7
8
9

Figure 2.1

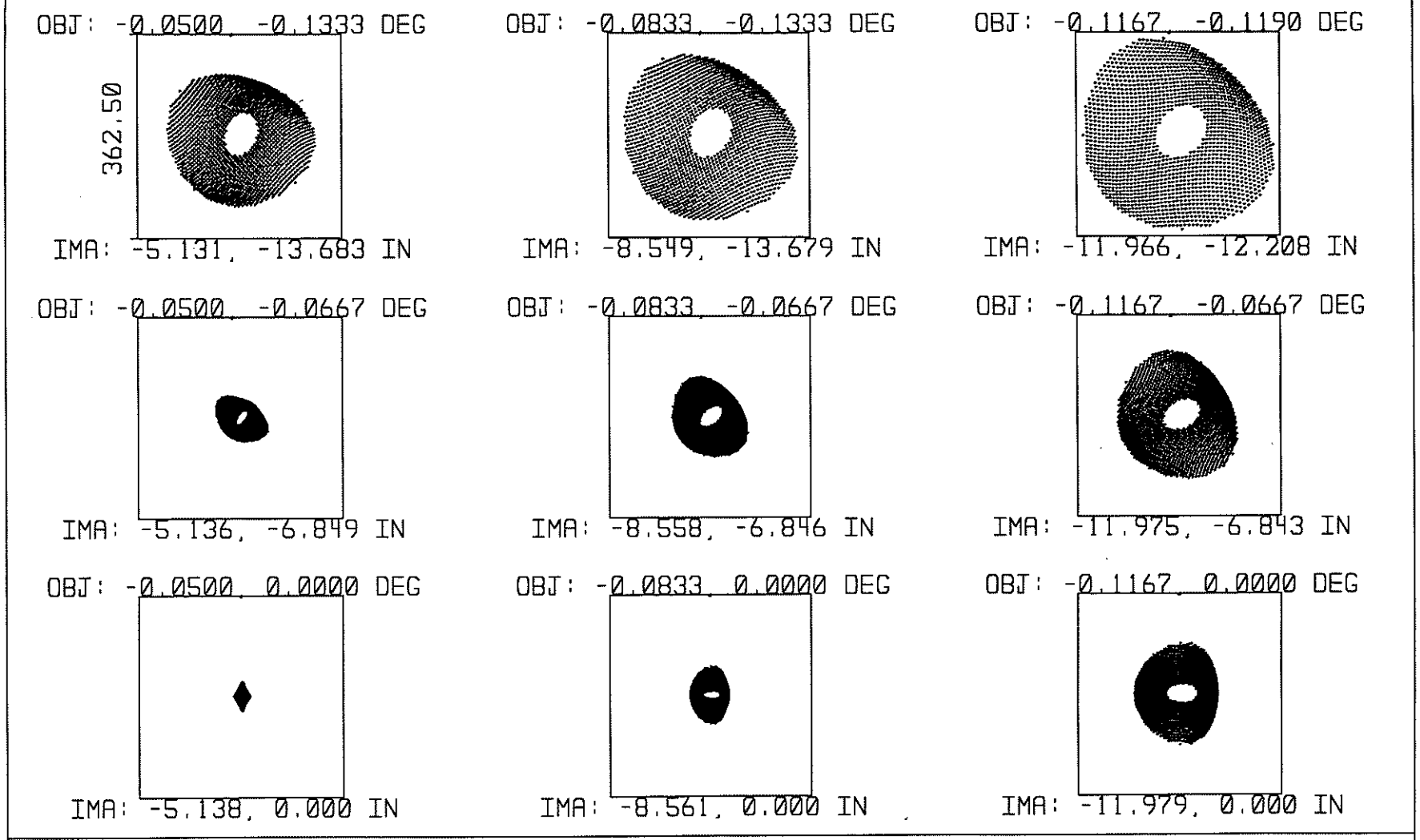

SPOT DIAGRAM

TELESCOPE AT NOMINAL FOCUS
MON APR 3 1995 UNITS ARE MICRONS.

FIELD	:	1	2	3	4	5	6	7	8	9
RMS RADIUS	:	90.87	110.65	124.24	31.54	51.29	80.98	12.27	31.54	61.19
GEO RADIUS	:	134.29	162.97	182.63	51.83	78.80	120.23	26.09	51.82	92.38

BOX WIDTH : 362.5 REFERENCE : CENTROID

Figure 3.1

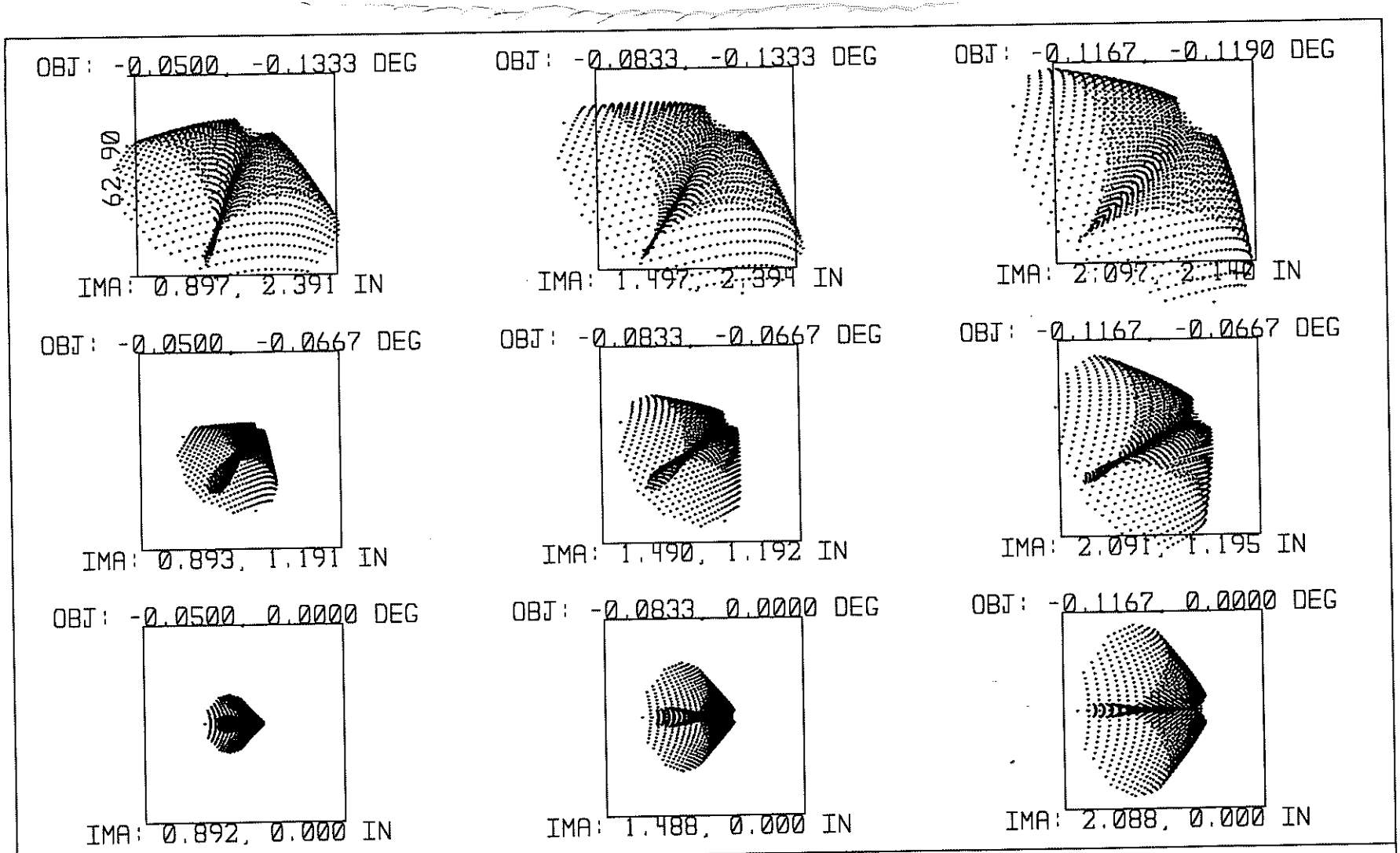

SPOT DIAGRAM

IMAGING / NOMINAL FOCUS / CONIC = -0.80
MON APR 3 1995 UNITS ARE MICRONS.

FIELD	1	2	3	4	5	6	7	8	9
RMS RADIUS :	18.34	21.31	23.34	8.87	12.20	16.84	4.93	8.87	13.77
GEO RADIUS :	38.42	44.33	48.03	20.00	26.34	35.49	12.63	19.97	29.30

BOX WIDTH : 0.5 ARCSEC REFERENCE : CENTROID

Figure 3.2

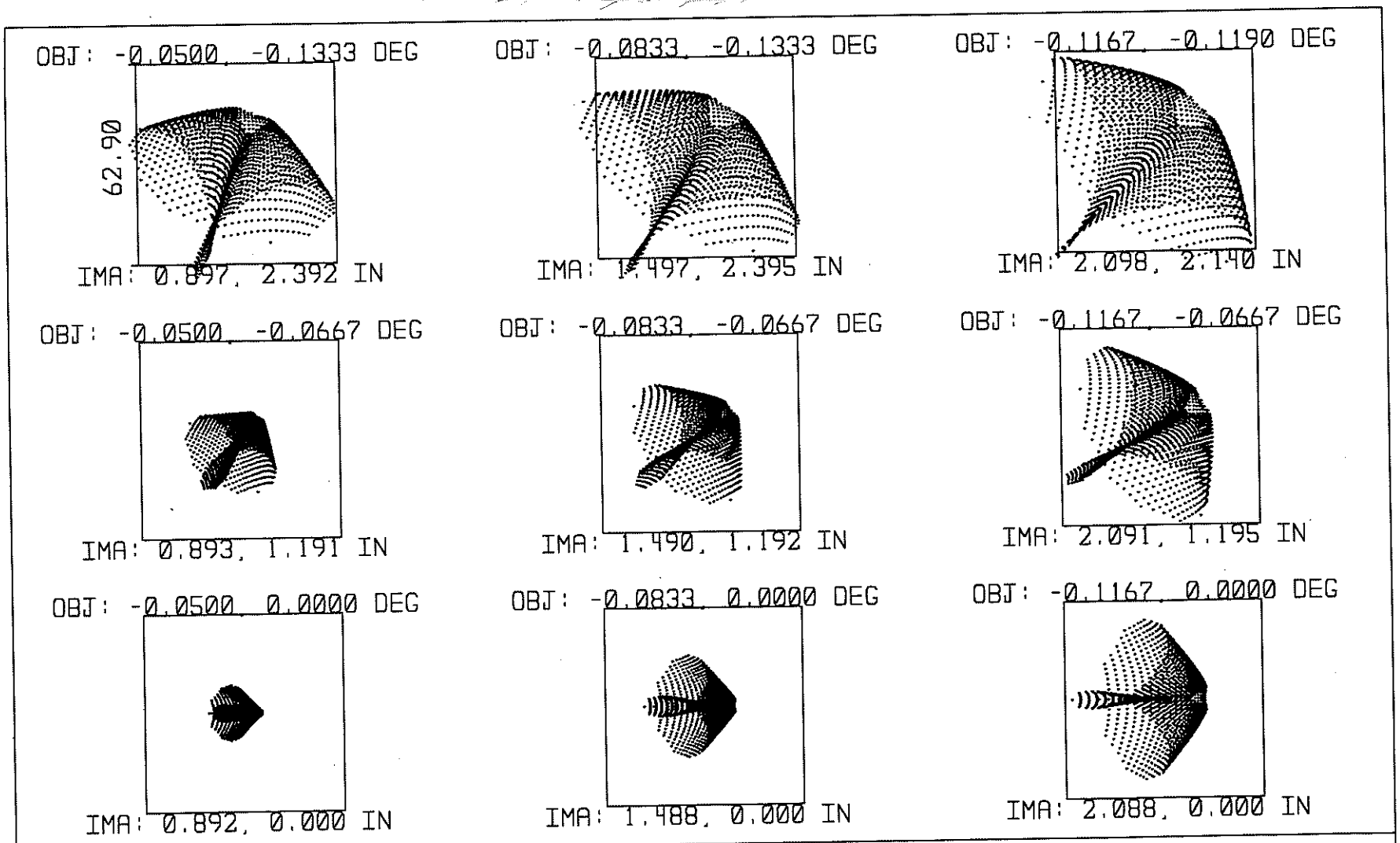

SPOT DIAGRAM

IMAGING / NOMINAL FOCUS / CONIC = -0.75
MON APR 3 1995 UNITS ARE MICRONS.

FIELD	:	1	2	3	4	5	6	7	8	9
RMS RADIUS	:	17.63	20.49	22.44	8.53	11.73	16.19	4.74	8.53	13.24
GEO RADIUS	:	37.45	42.52	45.46	19.13	26.06	34.45	11.13	19.13	29.19

BOX WIDTH : 0.5 ARCSEC REFERENCE : CENTROID

Figure 3.3

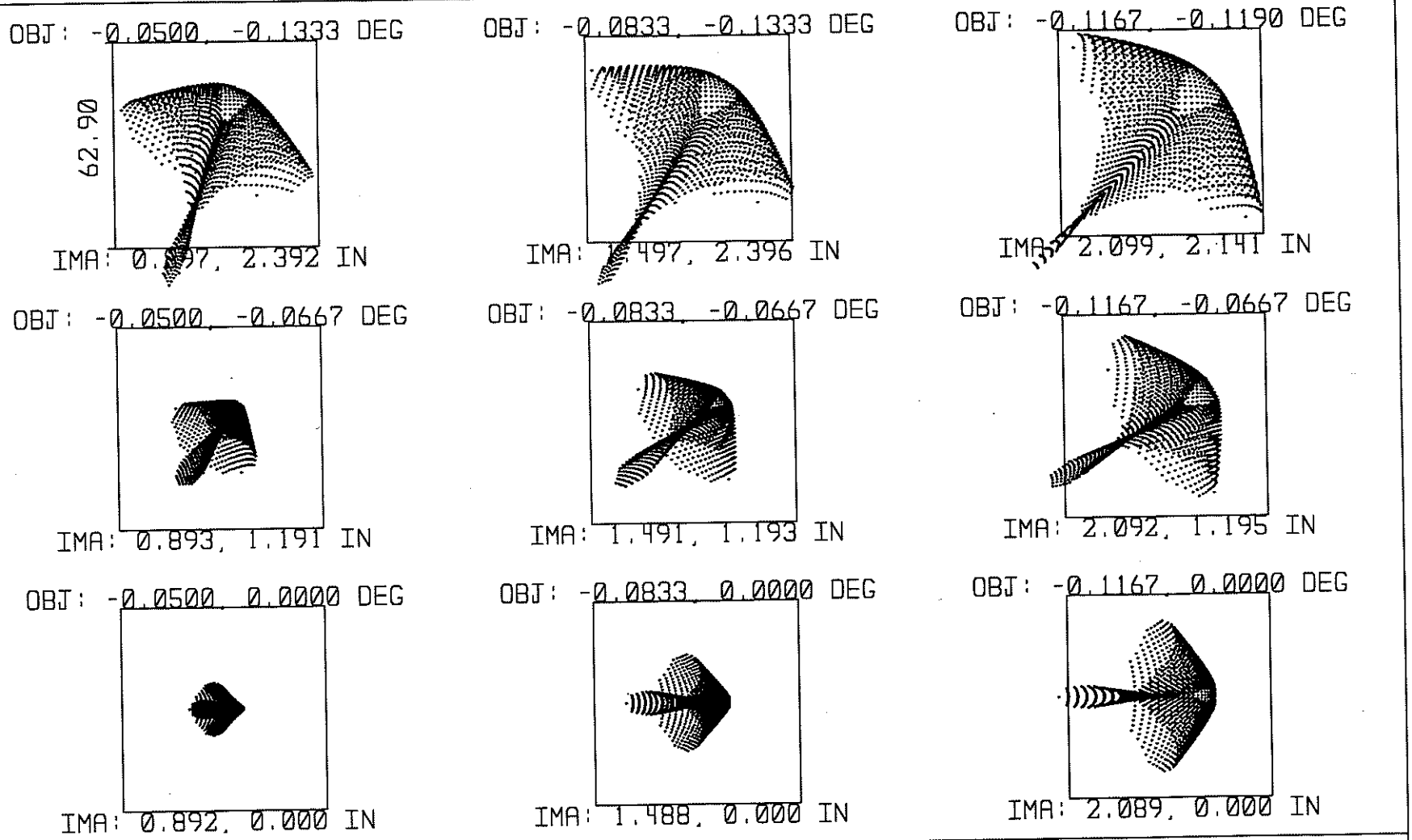

SPOT DIAGRAM

IMAGING / NOMINAL FOCUS / CONIC = -0.70
MON APR 3 1995 UNITS ARE MICRONS.

FIELD	:	1	2	3	4	5	6	7	8	9
RMS RADIUS	:	18.23	21.35	23.48	8.51	11.88	16.66	4.64	8.51	13.49
GEO RADIUS	:	45.34	52.28	56.48	21.60	30.29	41.38	10.89	21.61	34.32

BOX WIDTH : 0.5 ARCSEC REFERENCE : CENTROID

Figure 3.4

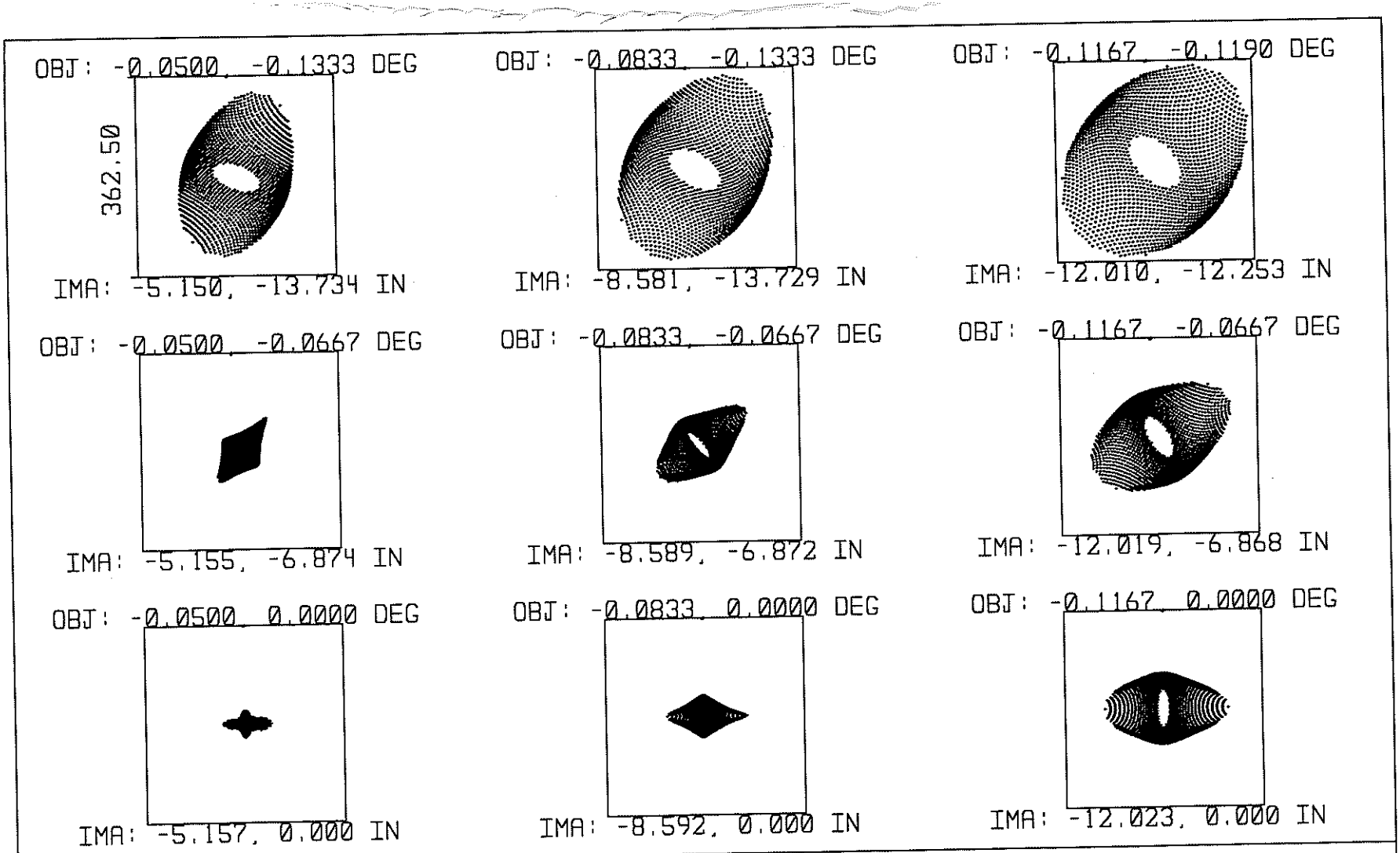

SPOT DIAGRAM

TELESCOPE WITH 3" PULLBACK
MON APR 3 1995 UNITS ARE MICRONS.

FIELD	:	1	2	3	4	5	6	7	8	9
RMS RADIUS	:	91.92	111.56	125.08	34.17	52.99	82.13	17.90	34.17	62.65
GEO RADIUS	:	156.77	181.65	197.76	75.90	104.06	143.41	46.07	75.90	117.75

BOX WIDTH : 0.5 ARCSEC REFERENCE : CENTROID

Figure 3.5

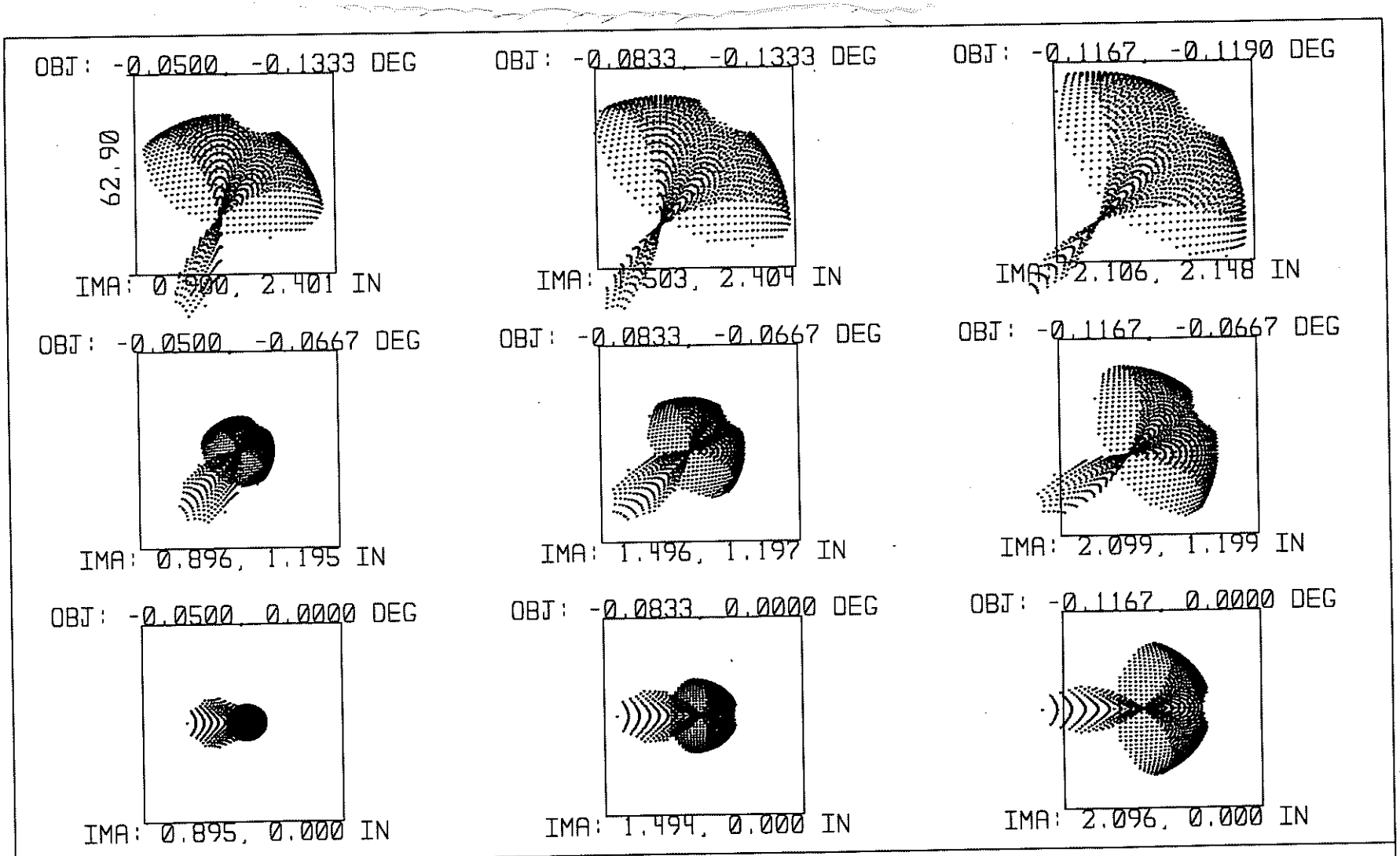

SPOT DIAGRAM

IMAGING / 3" PULLBACK / CONIC = -0.75
MON APR 3 1995 UNITS ARE MICRONS.

FIELD	:	1	2	3	4	5	6	7	8	9
RMS RADIUS	:	18.48	21.36	23.33	9.30	12.52	17.02	5.58	9.30	14.05
GEO RADIUS	:	47.02	52.44	55.55	27.43	34.84	43.80	17.72	27.43	38.19

BOX WIDTH : 0.5 ARCSEC REFERENCE : CENTROID

Figure 3.6

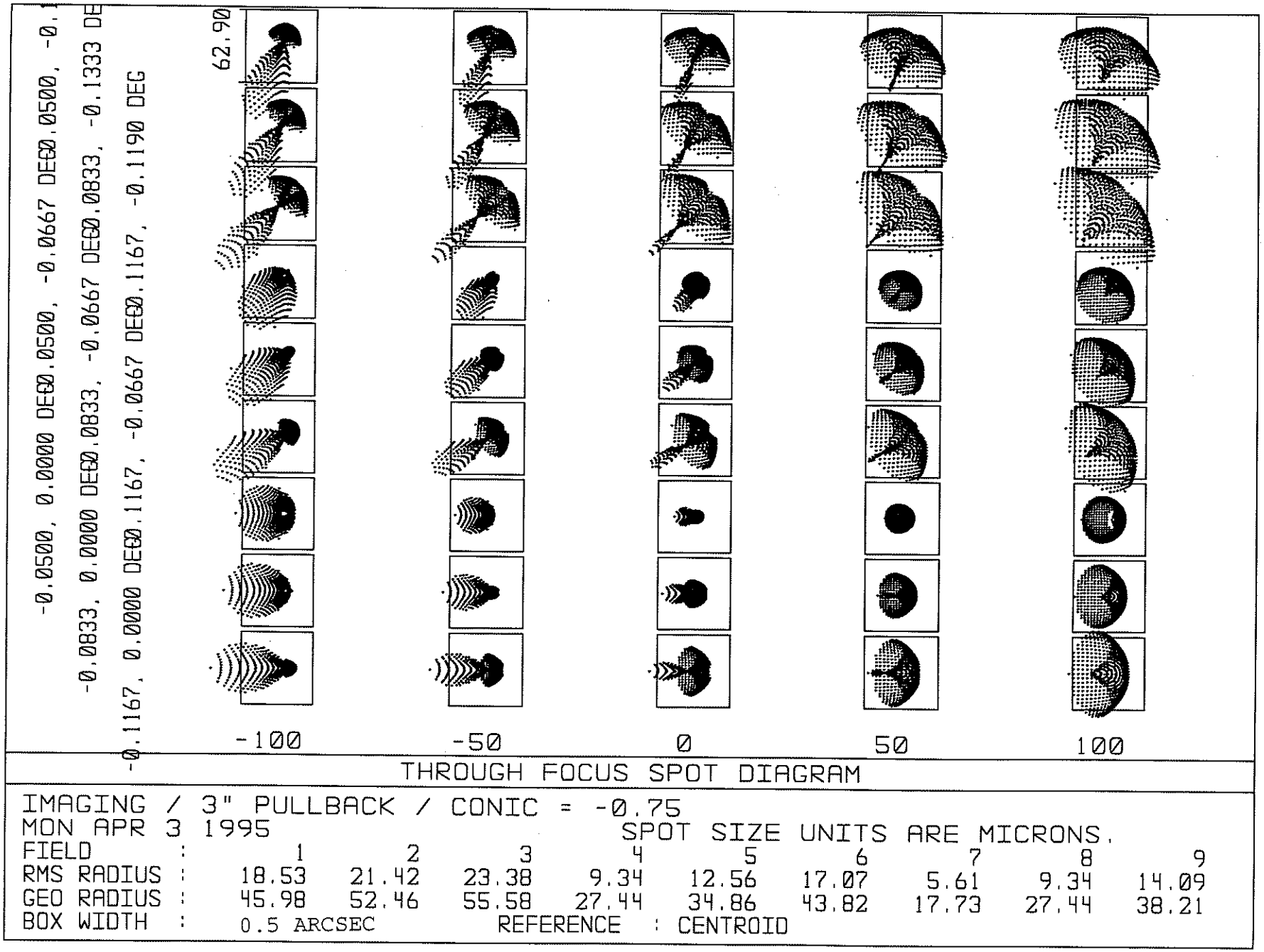
-0.0500, 0.0000 DEG 0.0500, -0.0667 DEG 0.0500, -0.
-0.0833, 0.0000 DEG 0.0833, -0.0667 DEG 0.0833, -0.1333 DE
-0.1167, 0.0000 DEG 0.1167, -0.0667 DEG 0.1167, -0.1190 DEG
62.90
-100
-50
0
50
100
THROUGH FOCUS SPOT DIAGRAM
IMAGING / 3" PULLBACK / CONIC = -0.75
MON APR 3 1995
SPOT SIZE UNITS ARE MICRONS.
FIELD : 1 2 3 4 5 6 7 8 9
RMS RADIUS : 18.53 21.42 23.38 9.34 12.56 17.07 5.61 9.34 14.09
GEO RADIUS : 45.98 52.46 55.58 27.44 34.86 43.82 17.73 27.44 38.21
BOX WIDTH : 0.5 ARCSEC REFERENCE : CENTROID

Figure 3.7

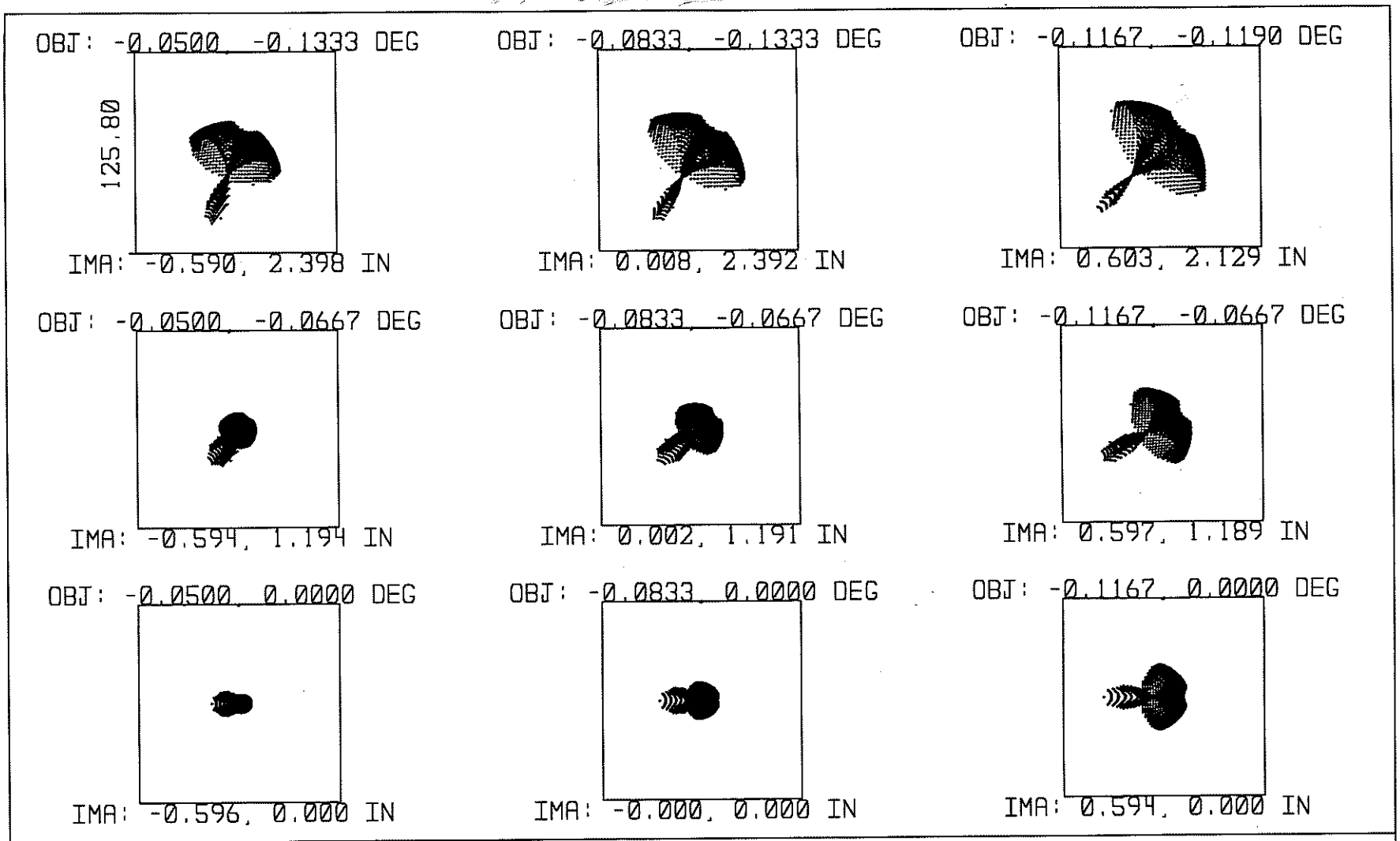

SPOT DIAGRAM

IMAGING / 3" PULLBACK / PARAXIAL CAMERA
TUE APR 4 1995 UNITS ARE MICRONS.

FIELD	:	1	2	3	4	5	6	7	8	9
RMS RADIUS	:	18.46	21.22	23.04	9.28	12.42	16.80	5.57	9.23	13.86
GEO RADIUS	:	46.74	51.72	54.45	27.29	34.43	42.98	17.68	27.16	37.52

BOX WIDTH : 1.0 ARCSEC REFERENCE : CENTROID

Figure 3.8

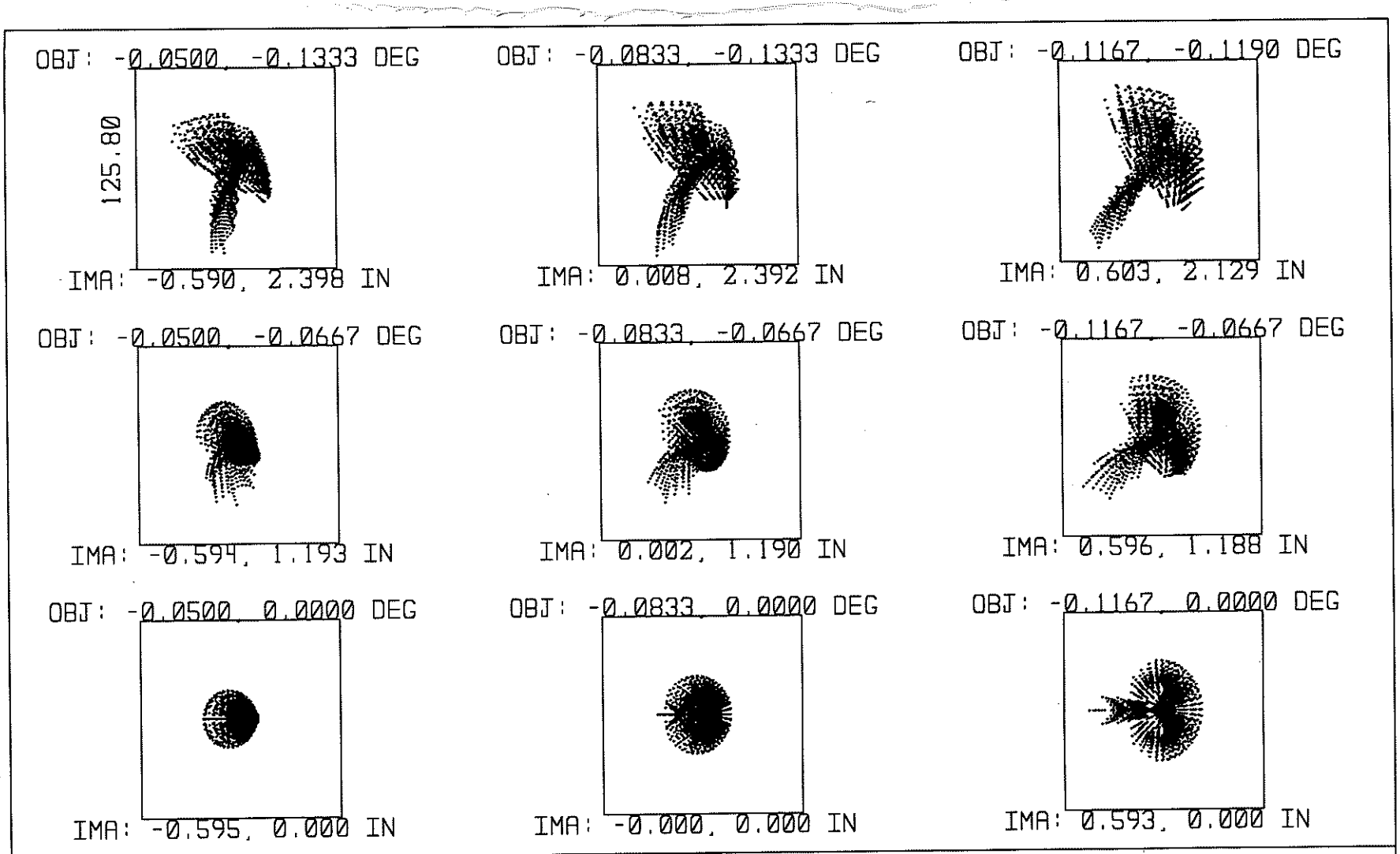

SPOT DIAGRAM

IMAGING / 3" PULLBACK / 3761 CAMERA / V BAND
TUE APR 4 1995 UNITS ARE MICRONS.

FIELD	:	1	2	3	4	5	6	7	8	9
RMS RADIUS	:	19.05	21.69	23.76	12.64	15.32	19.21	9.45	12.93	16.90
GEO RADIUS	:	54.57	62.70	66.27	38.26	45.02	58.70	23.40	28.64	46.67

BOX WIDTH : 1.0 ARCSEC REFERENCE : CENTROID

Figure 3.9

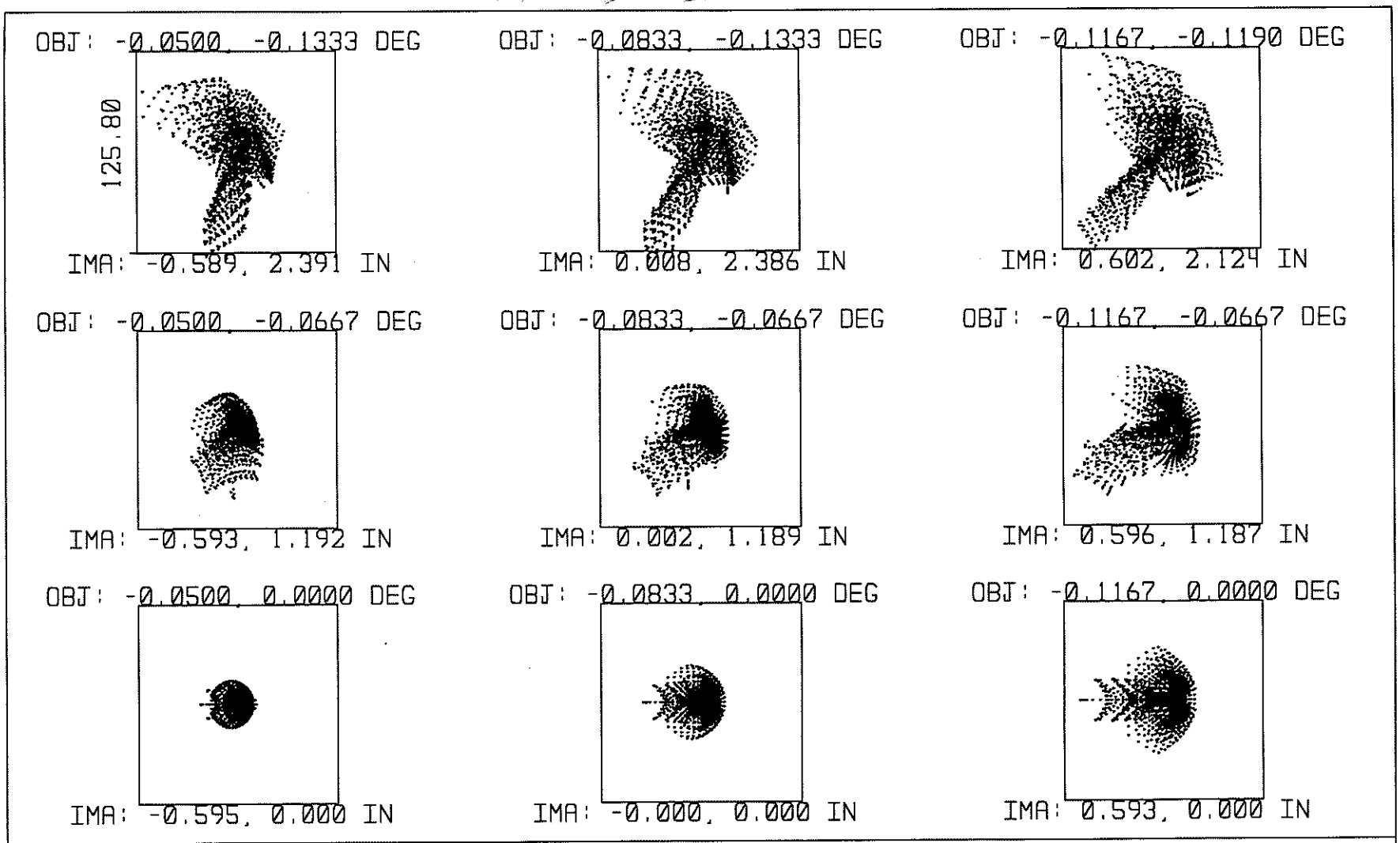

SPOT DIAGRAM

IMAGING / 3" PULLBACK / 3761 CAMERA / B BAND
TUE APR 4 1995 UNITS ARE MICRONS.

FIELD	:	1	2	3	4	5	6	7	8	9
RMS RADIUS	:	23.78	25.53	26.50	13.07	15.42	19.64	7.41	10.99	16.03
GEO RADIUS	:	70.31	75.07	76.26	44.53	50.69	64.34	24.26	36.21	52.97

BOX WIDTH : 1.0 ARCSEC REFERENCE : CENTROID

Figure 3.10

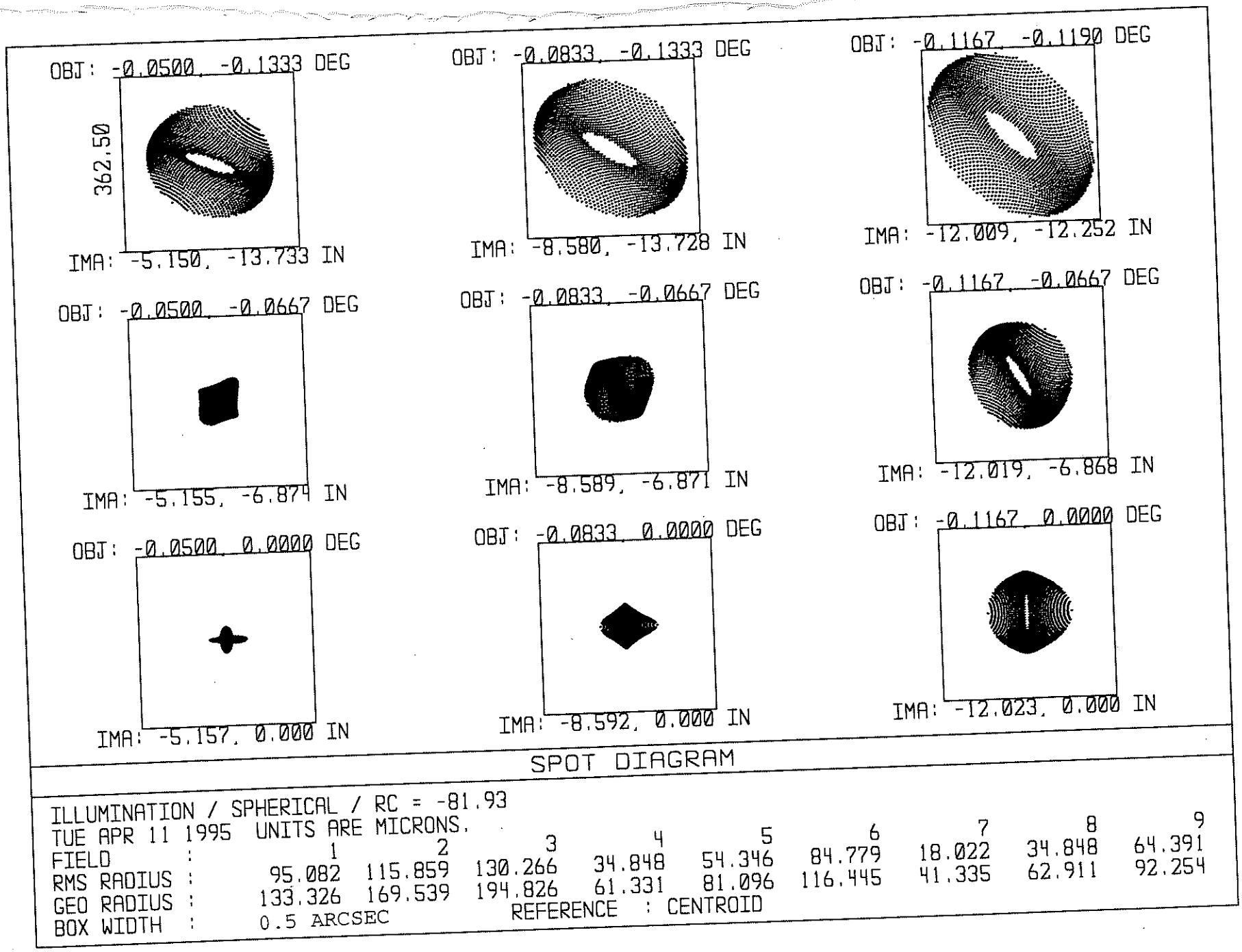
OBJ: -0.0500, -0.1333 DEG
362.50
IMA: -5.150, -13.733 IN
OBJ: -0.0833, -0.1333 DEG
IMA: -8.580, -13.728 IN
OBJ: -0.1167, -0.1190 DEG
IMA: -12.009, -12.252 IN
OBJ: -0.0500, -0.0667 DEG
IMA: -5.155, -6.874 IN
OBJ: -0.0833, -0.0667 DEG
IMA: -8.589, -6.871 IN
OBJ: -0.1167, -0.0667 DEG
IMA: -12.019, -6.868 IN
OBJ: -0.0500, 0.0000 DEG
IMA: -5.157, 0.000 IN
OBJ: -0.0833, 0.0000 DEG
IMA: -8.592, 0.000 IN
OBJ: -0.1167, 0.0000 DEG
IMA: -12.023, 0.000 IN
SPOT DIAGRAM
ILLUMINATION / SPHERICAL / RC = -81.93
TUE APR 11 1995 UNITS ARE MICRONS.
FIELD : 1 2 3 4 5 6 7 8 9
RMS RADIUS : 95.082 115.859 130.266 34.848 54.346 84.779 18.022 34.848 64.391
GEO RADIUS : 133.326 169.539 194.826 61.331 81.096 116.445 41.335 62.911 92.254
BOX WIDTH : 0.5 ARCSEC REFERENCE : CENTROID

Figure 4.1

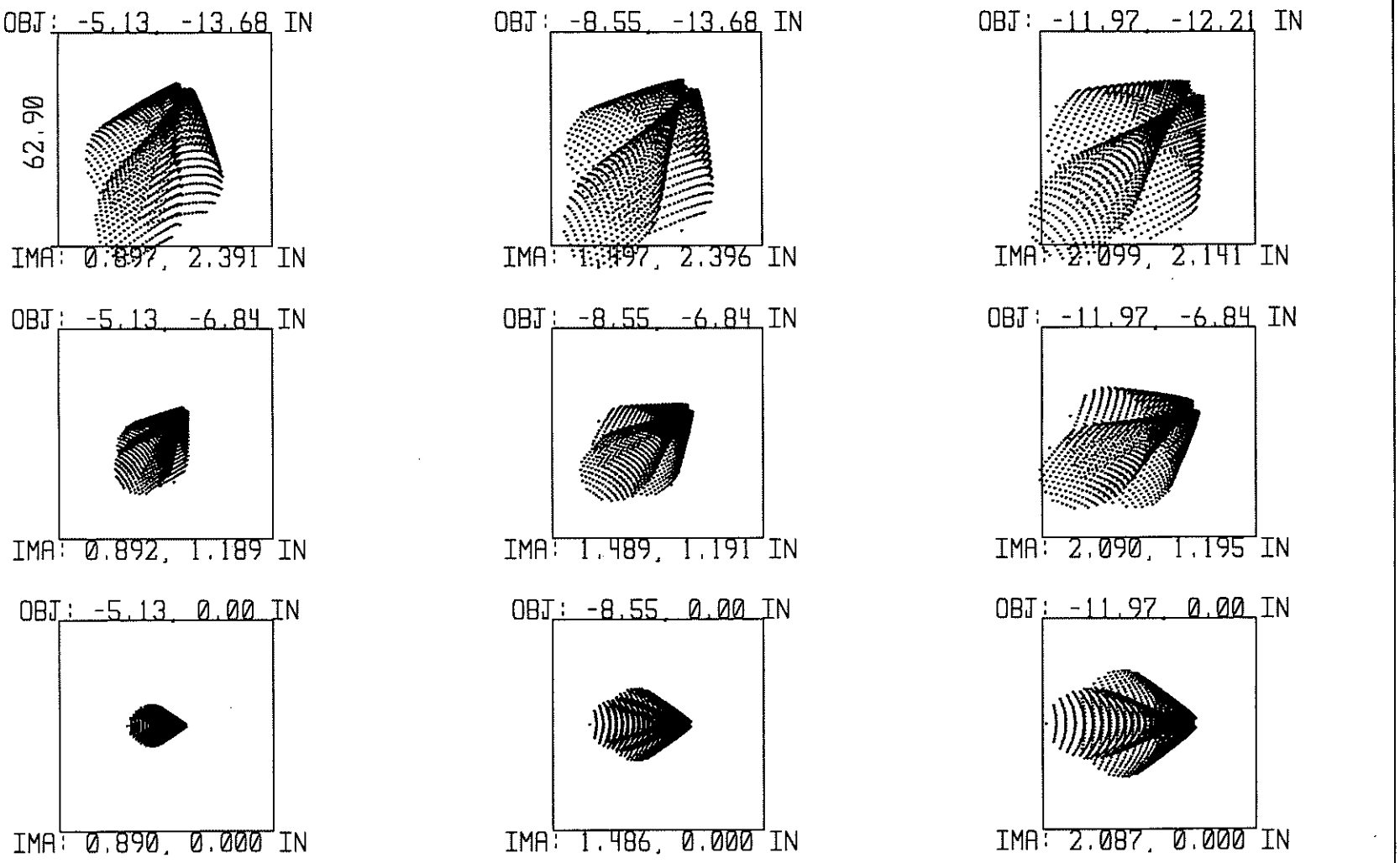

SPOT DIAGRAM

SLIT IMAGES / SPHERICAL SURFACE / RC = -81.93
TUE APR 11 1995 UNITS ARE MICRONS.

FIELD	:	1	2	3	4	5	6	7	8	9
RMS RADIUS	:	14.045	15.777	16.919	7.789	10.160	13.138	4.588	7.789	11.207
GEO RADIUS	:	38.011	42.426	45.104	20.150	26.882	35.228	11.484	20.559	30.450

BOX WIDTH : 0.5 ARCSEC REFERENCE : CENTROID

Figure 4.2

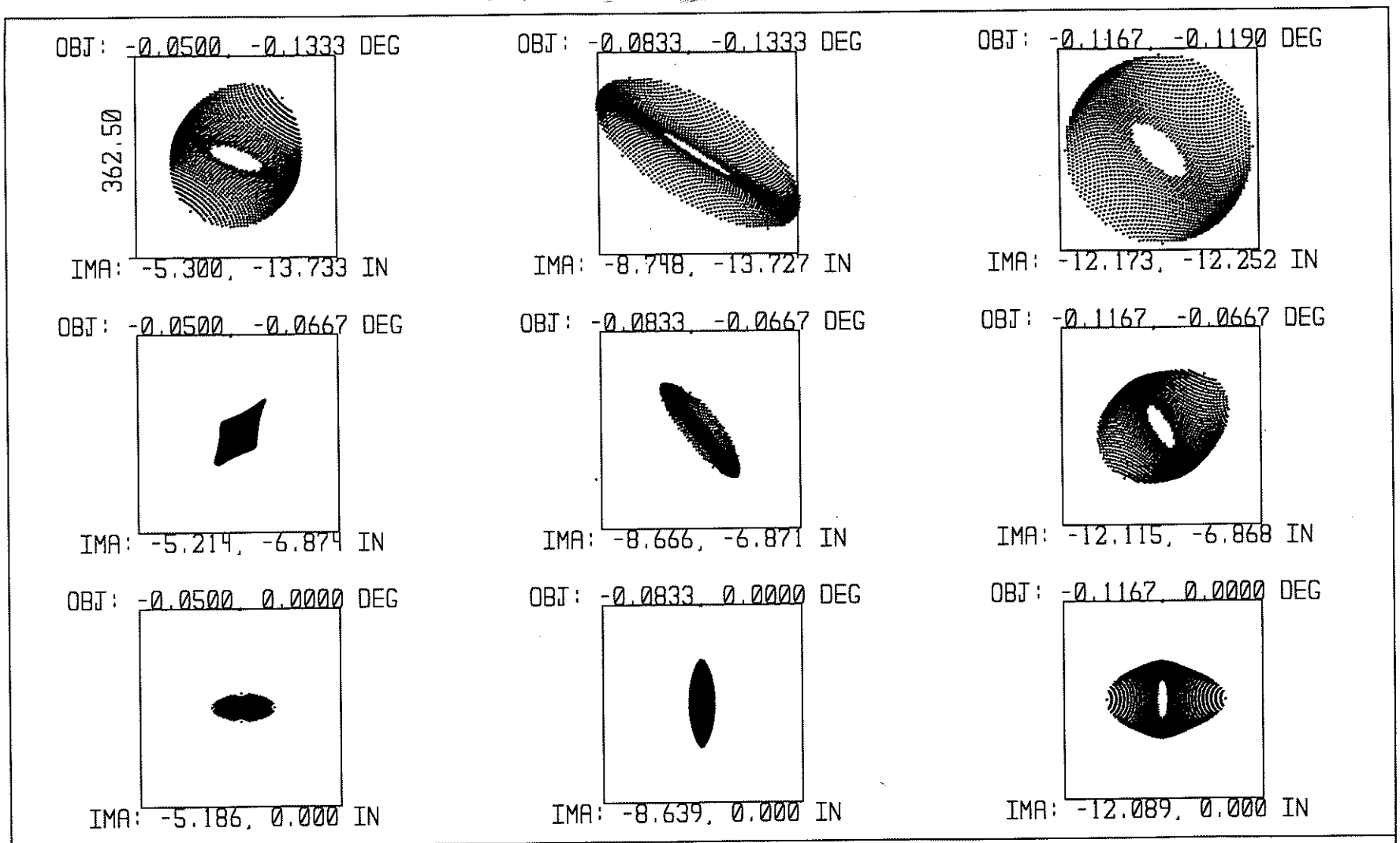

SPOT DIAGRAM

SLIT ILLUMINATION / CYLINDRICAL SURFACE
TUE APR 11 1995 UNITS ARE MICRONS.

FIELD	:	1	2	3	4	5	6	7	8	9
RMS RADIUS	:	92.736	127.205	126.373	34.414	69.630	82.378	20.580	52.385	62.641
GEO RADIUS	:	135.764	209.768	171.377	77.931	108.653	129.804	59.408	79.449	113.006

BOX WIDTH : 0.5 ARCSEC REFERENCE : CENTROID

Figure 4.3

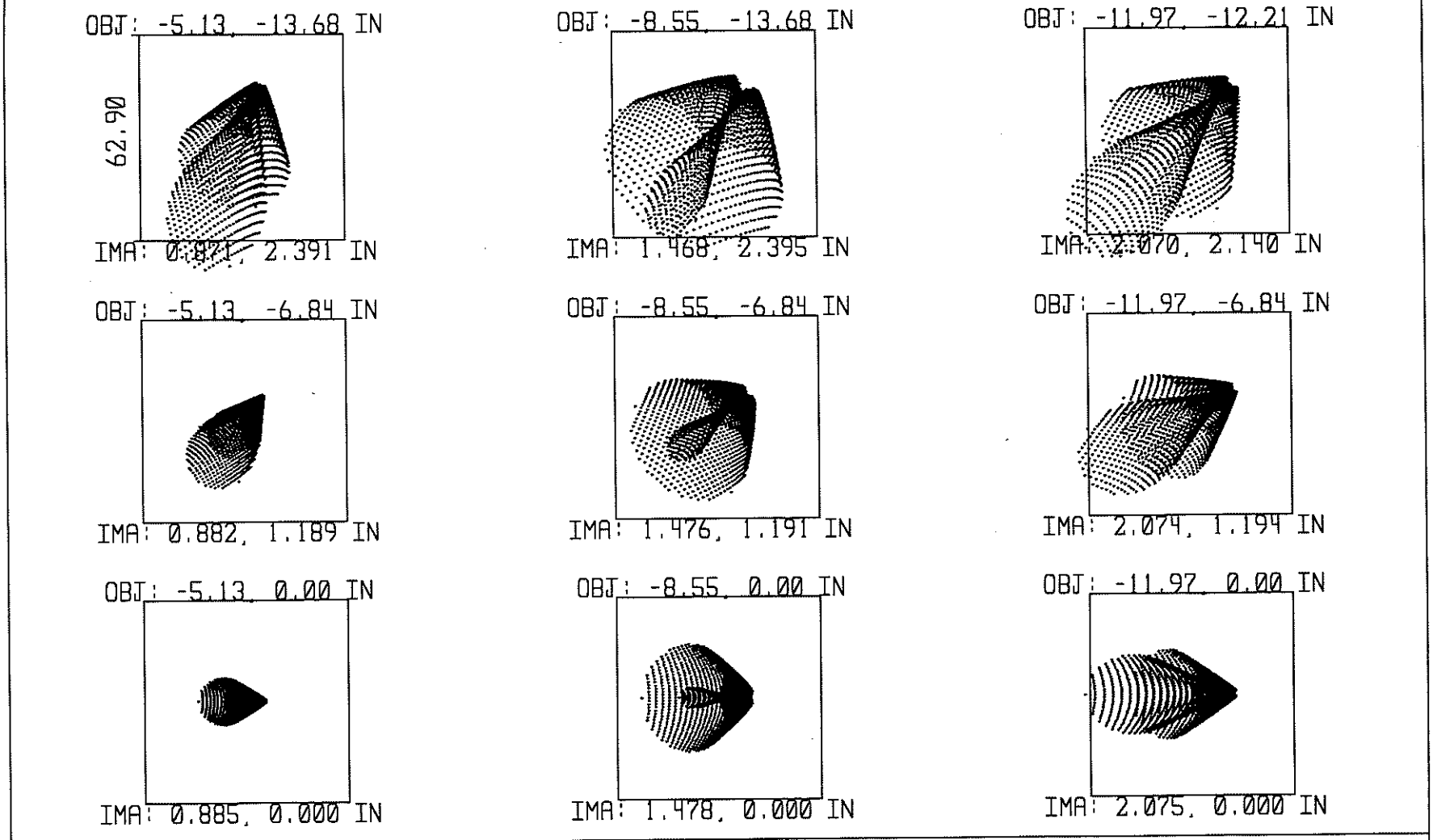

SPOT DIAGRAM

SLIT IMAGES / CYLINDRICAL SURFACE / YRC = -81.57
TUE APR 11 1995 UNITS ARE MICRONS.

FIELD	:	1	2	3	4	5	6	7	8	9
RMS RADIUS	:	14.397	16.504	16.970	8.189	11.492	13.260	5.170	9.517	11.386
GEO RADIUS	:	42.105	35.035	48.051	23.448	27.446	37.748	14.853	24.080	33.069

BOX WIDTH : 0.5 ARCSEC REFERENCE : CENTROID

Figure 4.4

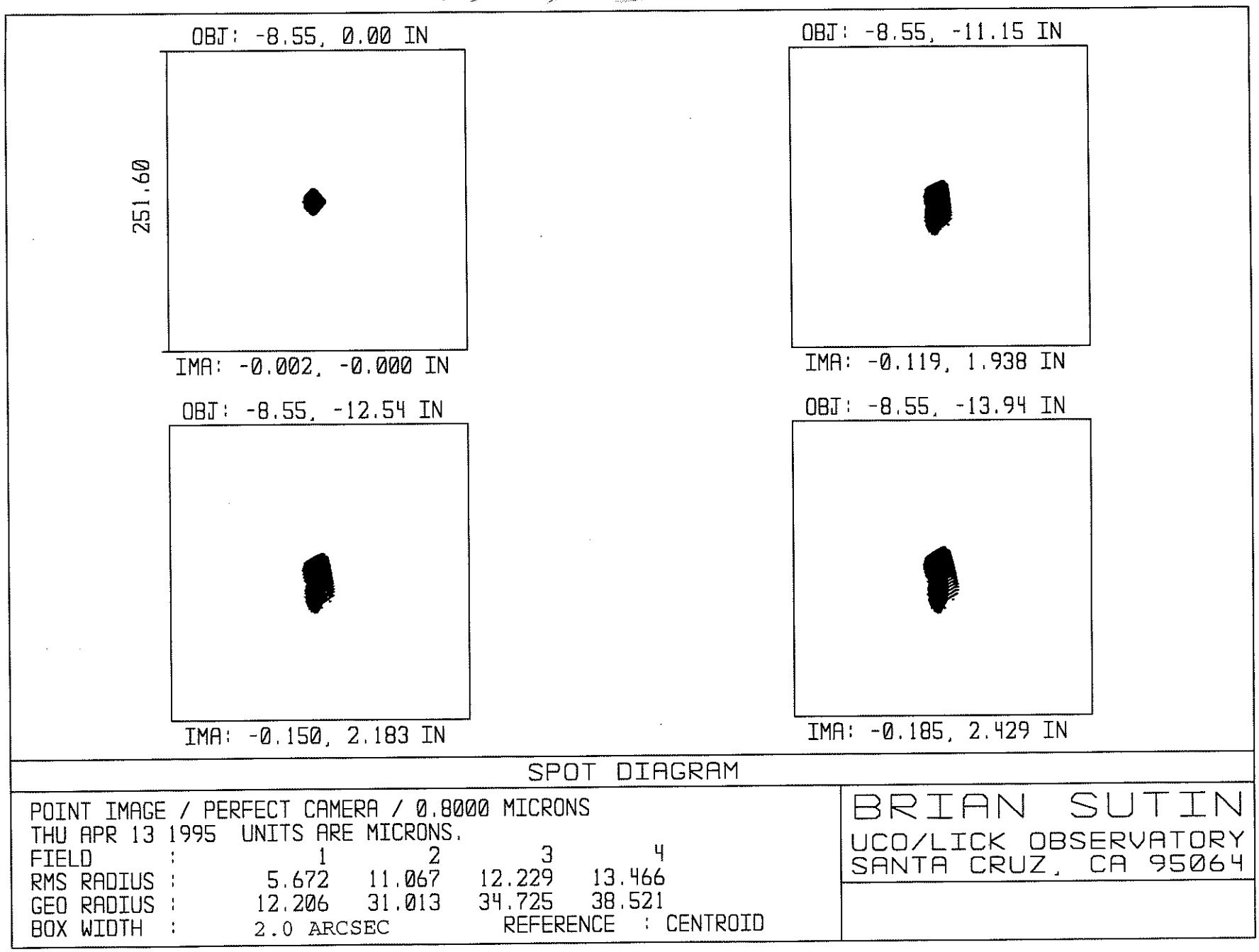
OBJ: -8.55, 0.00 IN
251.60
IMA: -0.002, -0.000 IN
OBJ: -8.55, -11.15 IN
IMA: -0.119, 1.938 IN
OBJ: -8.55, -12.54 IN
IMA: -0.150, 2.183 IN
OBJ: -8.55, -13.94 IN
IMA: -0.185, 2.429 IN
SPOT DIAGRAM
POINT IMAGE / PERFECT CAMERA / 0.8000 MICRONS
THU APR 13 1995 UNITS ARE MICRONS.
FIELD : 1 2 3 4
RMS RADIUS : 5.672 11.067 12.229 13.466
GEO RADIUS : 12.206 31.013 34.725 38.521
BOX WIDTH : 2.0 ARCSEC REFERENCE : CENTROID
BRIAN SUTIN
UCO/LICK OBSERVATORY
SANTA CRUZ, CA 95064

Figure 5.1

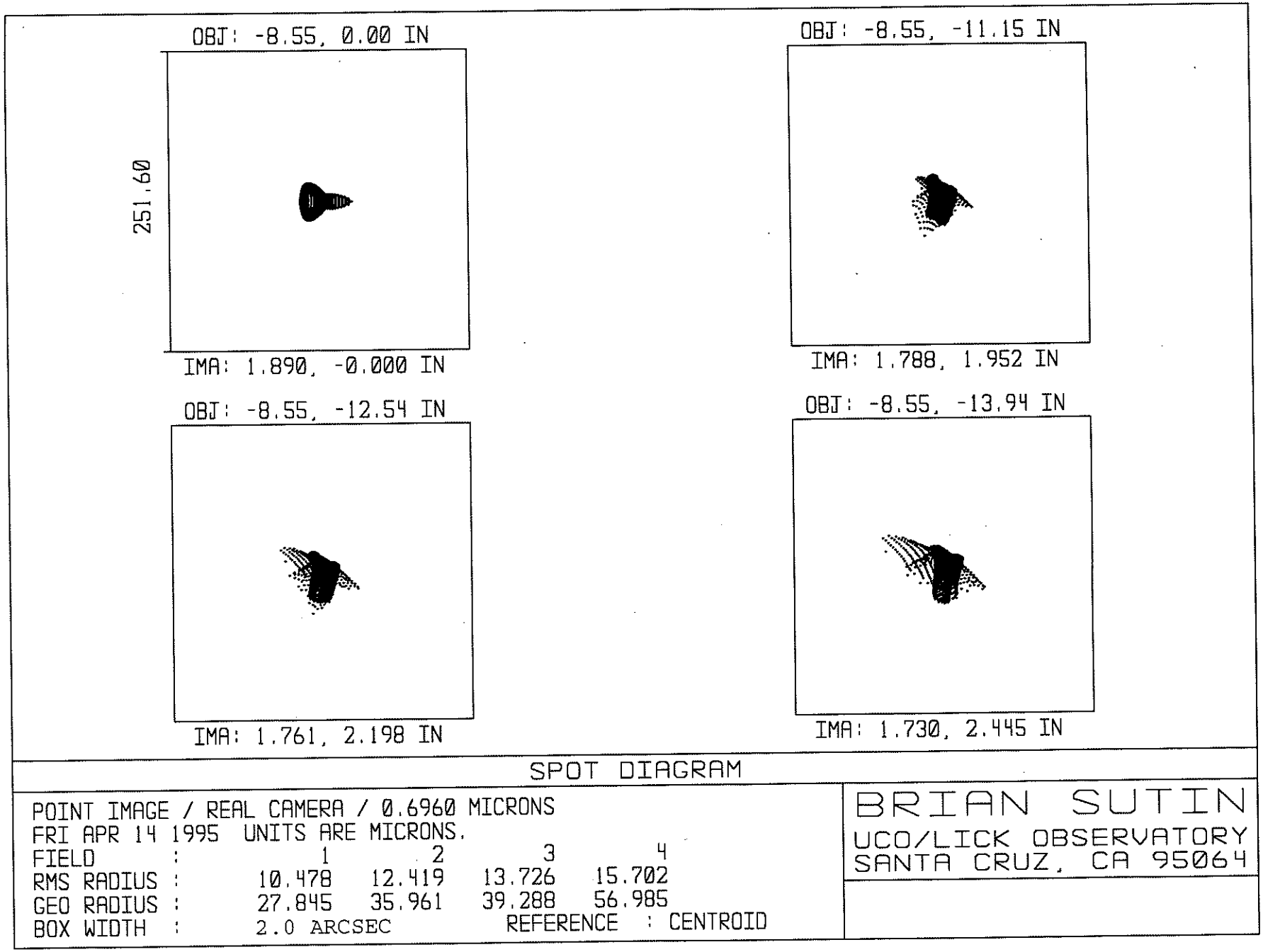
OBJ: -8.55, 0.00 IN
251.60
IMA: 1.890, -0.000 IN
OBJ: -8.55, -11.15 IN
IMA: 1.788, 1.952 IN
OBJ: -8.55, -12.54 IN
IMA: 1.761, 2.198 IN
OBJ: -8.55, -13.94 IN
IMA: 1.730, 2.445 IN
SPOT DIAGRAM
POINT IMAGE / REAL CAMERA / 0.6960 MICRONS
FRI APR 14 1995 UNITS ARE MICRONS.
FIELD : 1 2 3 4
RMS RADIUS : 10.478 12.419 13.726 15.702
GEO RADIUS : 27.845 35.961 39.288 56.985
BOX WIDTH : 2.0 ARCSEC REFERENCE : CENTROID
BRIAN SUTIN
UCO/LICK OBSERVATORY
SANTA CRUZ, CA 95064

Figure 5.2

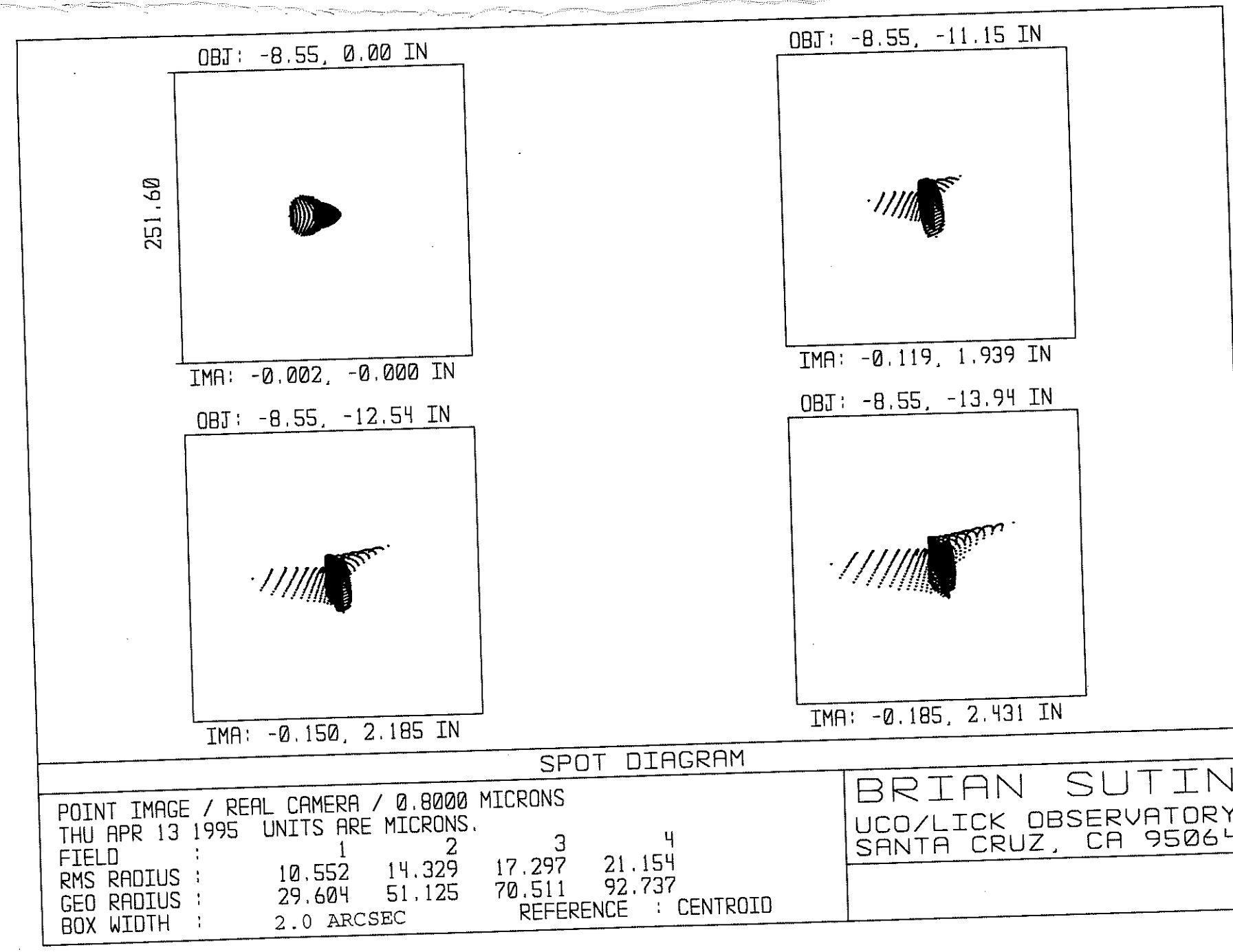
OBJ: -8.55, 0.00 IN
251.60
IMA: -0.002, -0.000 IN
OBJ: -8.55, -11.15 IN
IMA: -0.119, 1.939 IN
OBJ: -8.55, -12.54 IN
IMA: -0.150, 2.185 IN
OBJ: -8.55, -13.94 IN
IMA: -0.185, 2.431 IN
SPOT DIAGRAM
POINT IMAGE / REAL CAMERA / 0.8000 MICRONS
THU APR 13 1995 UNITS ARE MICRONS.
FIELD : 1 2 3 4
RMS RADIUS : 10.552 14.329 17.297 21.154
GEO RADIUS : 29.604 51.125 70.511 92.737
BOX WIDTH : 2.0 ARCSEC REFERENCE : CENTROID
BRIAN SUTIN
UCO/LICK OBSERVATORY
SANTA CRUZ, CA 95064

Figure 5.3

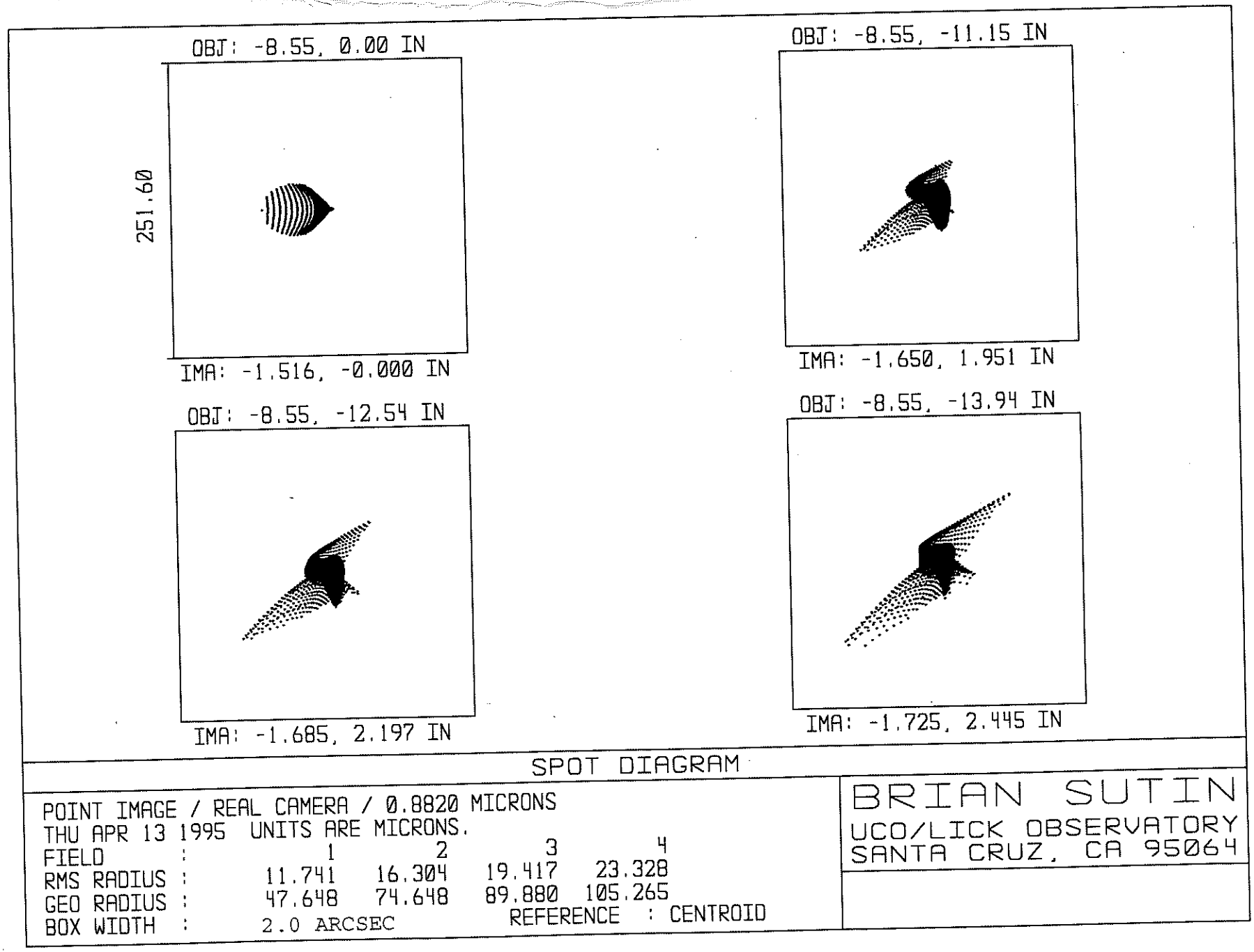
OBJ: -8.55, 0.00 IN
251.60
IMA: -1.516, -0.000 IN
OBJ: -8.55, -11.15 IN
IMA: -1.650, 1.951 IN
OBJ: -8.55, -12.54 IN
IMA: -1.685, 2.197 IN
OBJ: -8.55, -13.94 IN
IMA: -1.725, 2.445 IN
SPOT DIAGRAM
POINT IMAGE / REAL CAMERA / 0.8820 MICRONS
THU APR 13 1995 UNITS ARE MICRONS.
FIELD : 1 2 3 4
RMS RADIUS : 11.741 16.304 19.417 23.328
GEO RADIUS : 47.648 74.648 89.880 105.265
BOX WIDTH : 2.0 ARCSEC REFERENCE : CENTROID
BRIAN SUTIN
UCO/LICK OBSERVATORY
SANTA CRUZ, CA 95064

Figure 5.4

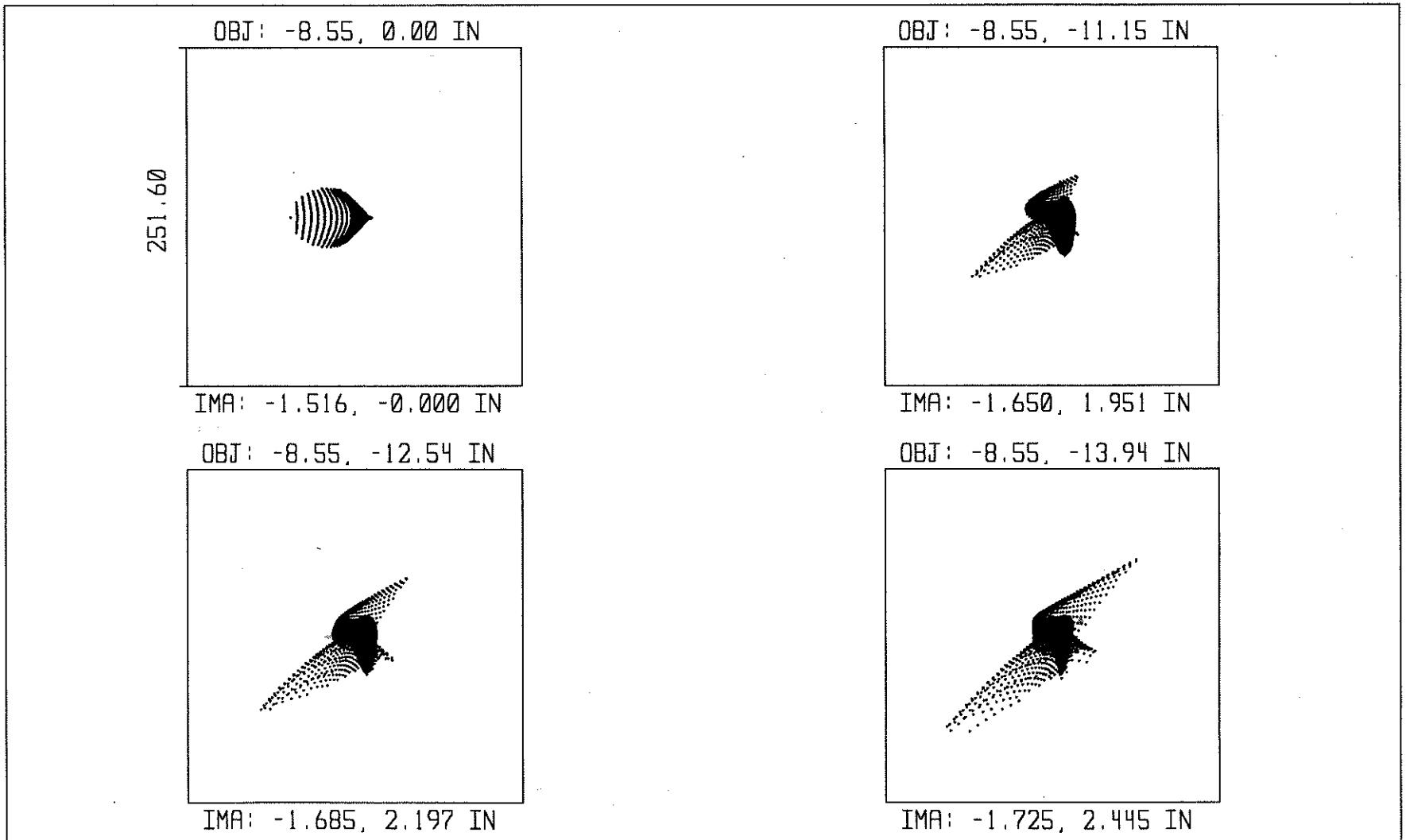
OBJ: -8.55, 0.00 IN
OBJ: -8.55, -11.15 IN
251.60
IMA: -1.516, -0.000 IN
IMA: -1.650, 1.951 IN
OBJ: -8.55, -12.54 IN
OBJ: -8.55, -13.94 IN
IMA: -1.685, 2.197 IN
IMA: -1.725, 2.445 IN
SPOT DIAGRAM
POINT IMAGE / REAL CAMERA / 0.8820 MICRONS
THU APR 13 1995 UNITS ARE MICRONS.
FIELD : 1 2 3 4
RMS RADIUS : 11.741 16.304 19.417 23.328
GEO RADIUS : 47.648 74.648 89.880 105.265
BOX WIDTH : 2.0 ARCSEC REFERENCE : CENTROID
BRIAN SUTIN
UCO/LICK OBSERVATORY
SANTA CRUZ, CA 95064

Figure 5.4

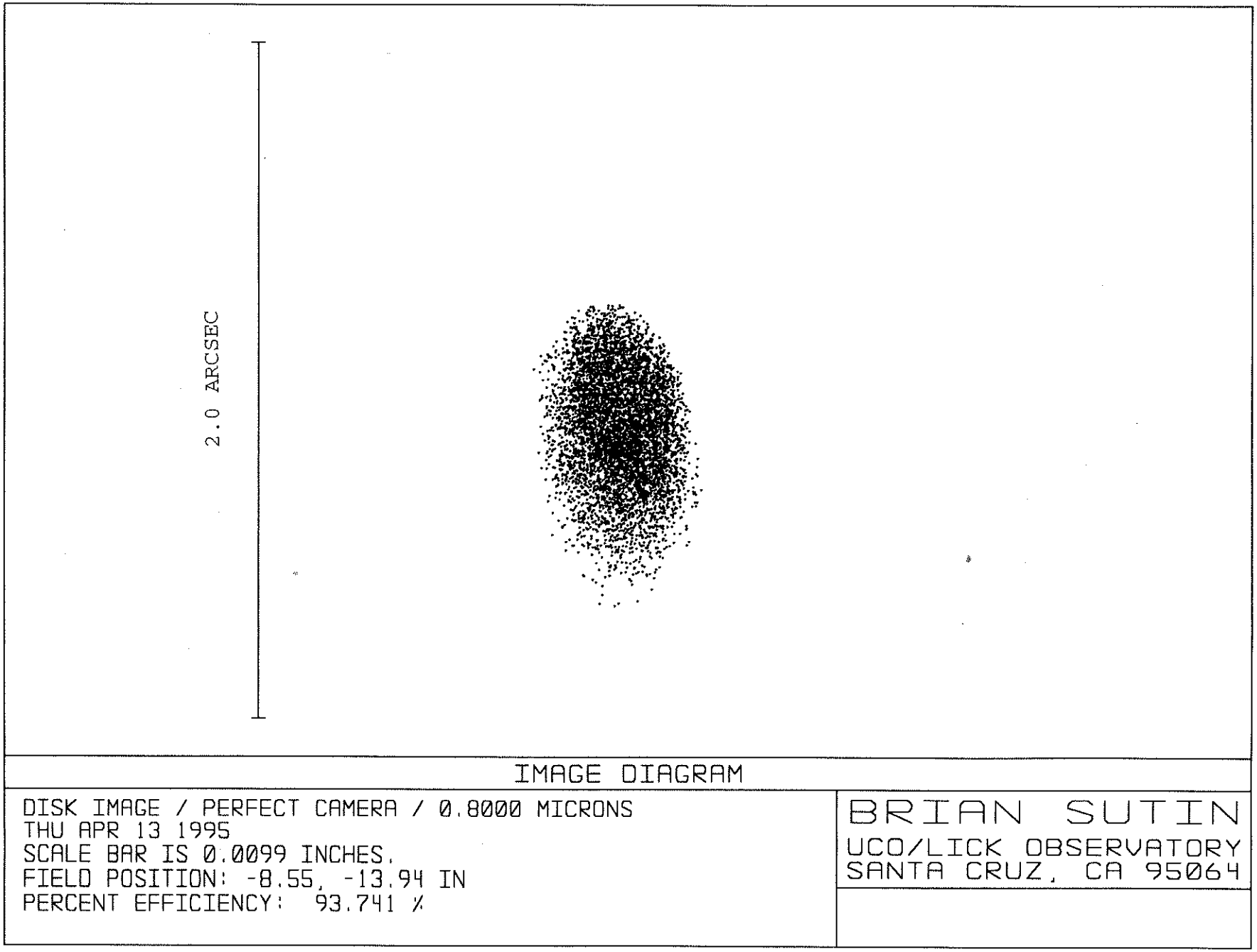
2.0 ARCSEC
IMAGE DIAGRAM
DISK IMAGE / PERFECT CAMERA / 0.8000 MICRONS
THU APR 13 1995
SCALE BAR IS 0.0099 INCHES.
FIELD POSITION: -8.55, -13.94 IN
PERCENT EFFICIENCY: 93.741 %
BRIAN SUTIN
UCO/LICK OBSERVATORY
SANTA CRUZ, CA 95064

Figure 5.5

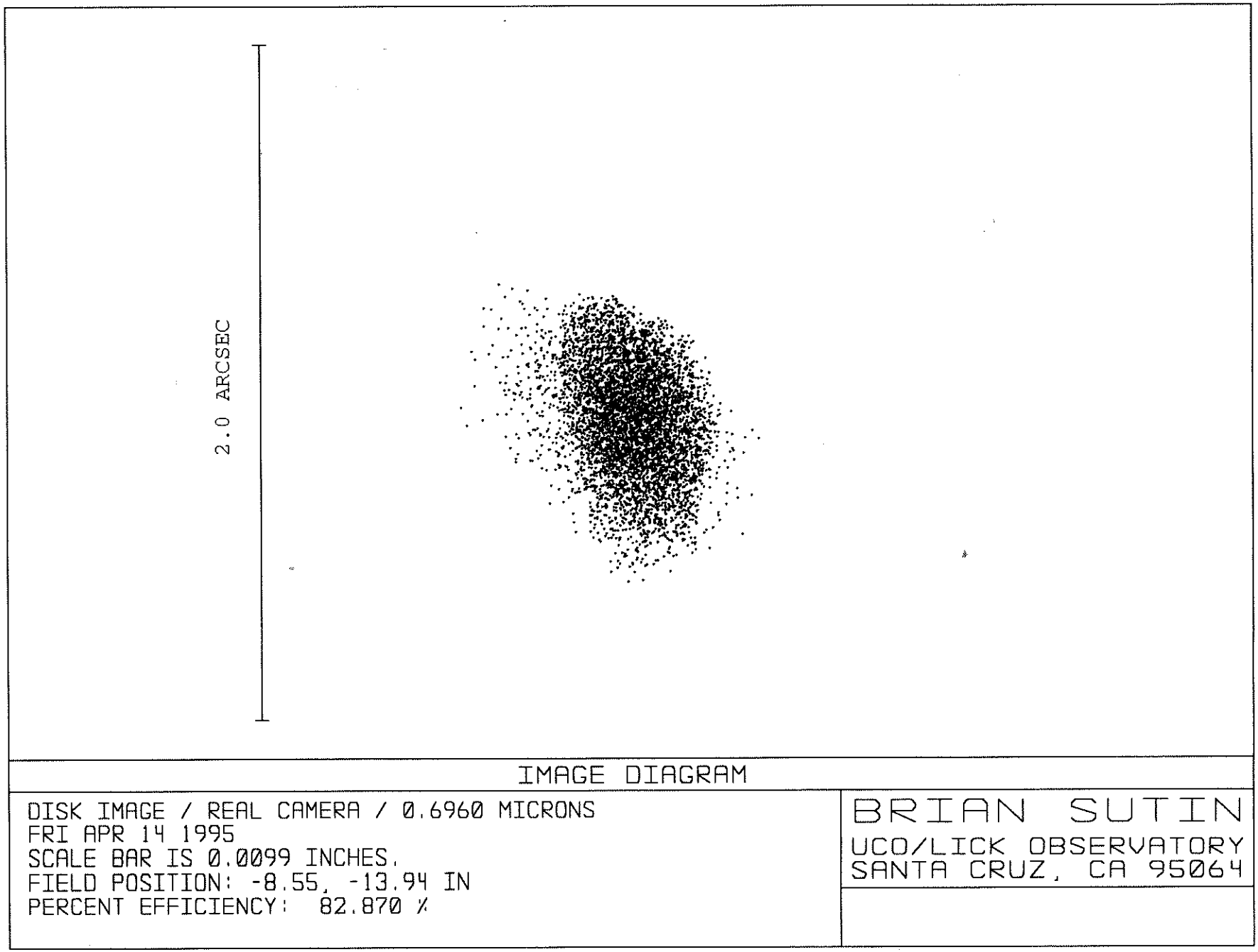
2.0 ARCSEC
IMAGE DIAGRAM
DISK IMAGE / REAL CAMERA / 0.6960 MICRONS
FRI APR 14 1995
SCALE BAR IS 0.0099 INCHES.
FIELD POSITION: -8.55, -13.94 IN
PERCENT EFFICIENCY: 82.870 %
BRIAN SUTIN
UCO/LICK OBSERVATORY
SANTA CRUZ, CA 95064

Figure 5.6

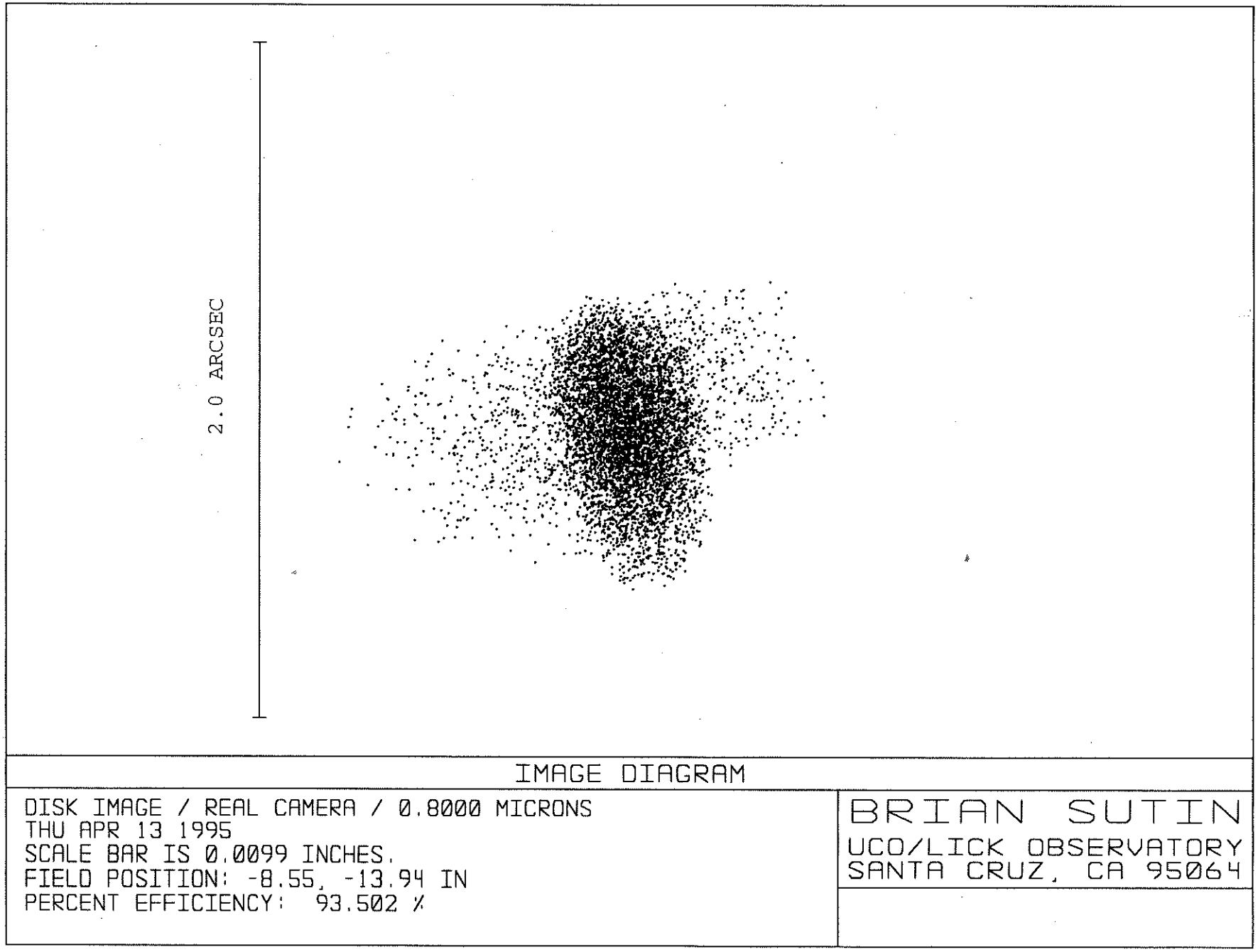
2.0 ARCSEC
IMAGE DIAGRAM
DISK IMAGE / REAL CAMERA / 0.8000 MICRONS
THU APR 13 1995
SCALE BAR IS 0.0099 INCHES.
FIELD POSITION: -8.55, -13.94 IN
PERCENT EFFICIENCY: 93.502 %
BRIAN SUTIN
UCO/LICK OBSERVATORY
SANTA CRUZ, CA 95064

Figure 5.7

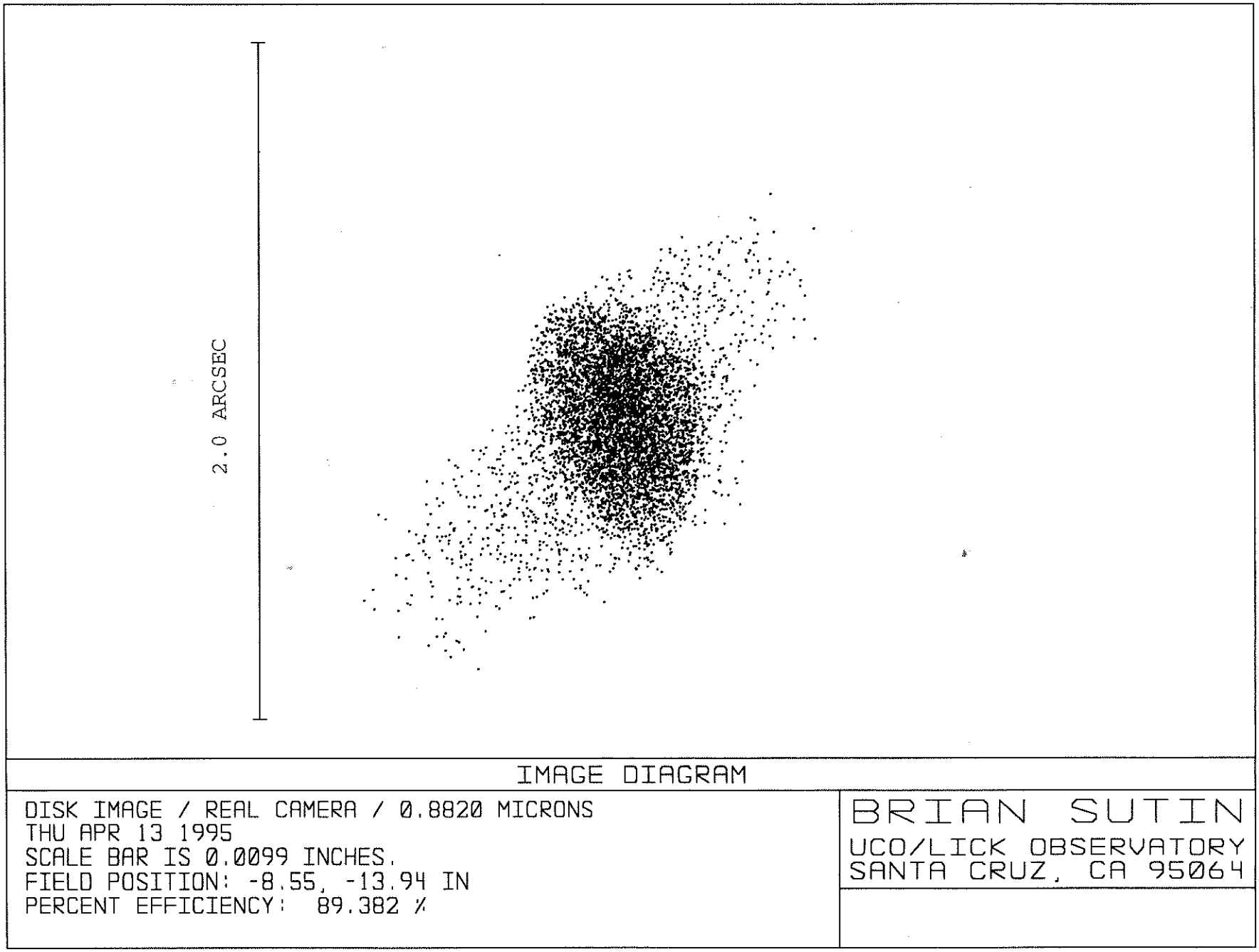
2.0 ARCSEC
IMAGE DIAGRAM
DISK IMAGE / REAL CAMERA / 0.8820 MICRONS
THU APR 13 1995
SCALE BAR IS 0.0099 INCHES.
FIELD POSITION: -8.55, -13.94 IN
PERCENT EFFICIENCY: 89.382 %
BRIAN SUTIN
UCO/LICK OBSERVATORY
SANTA CRUZ, CA 95064

Figure 5.8

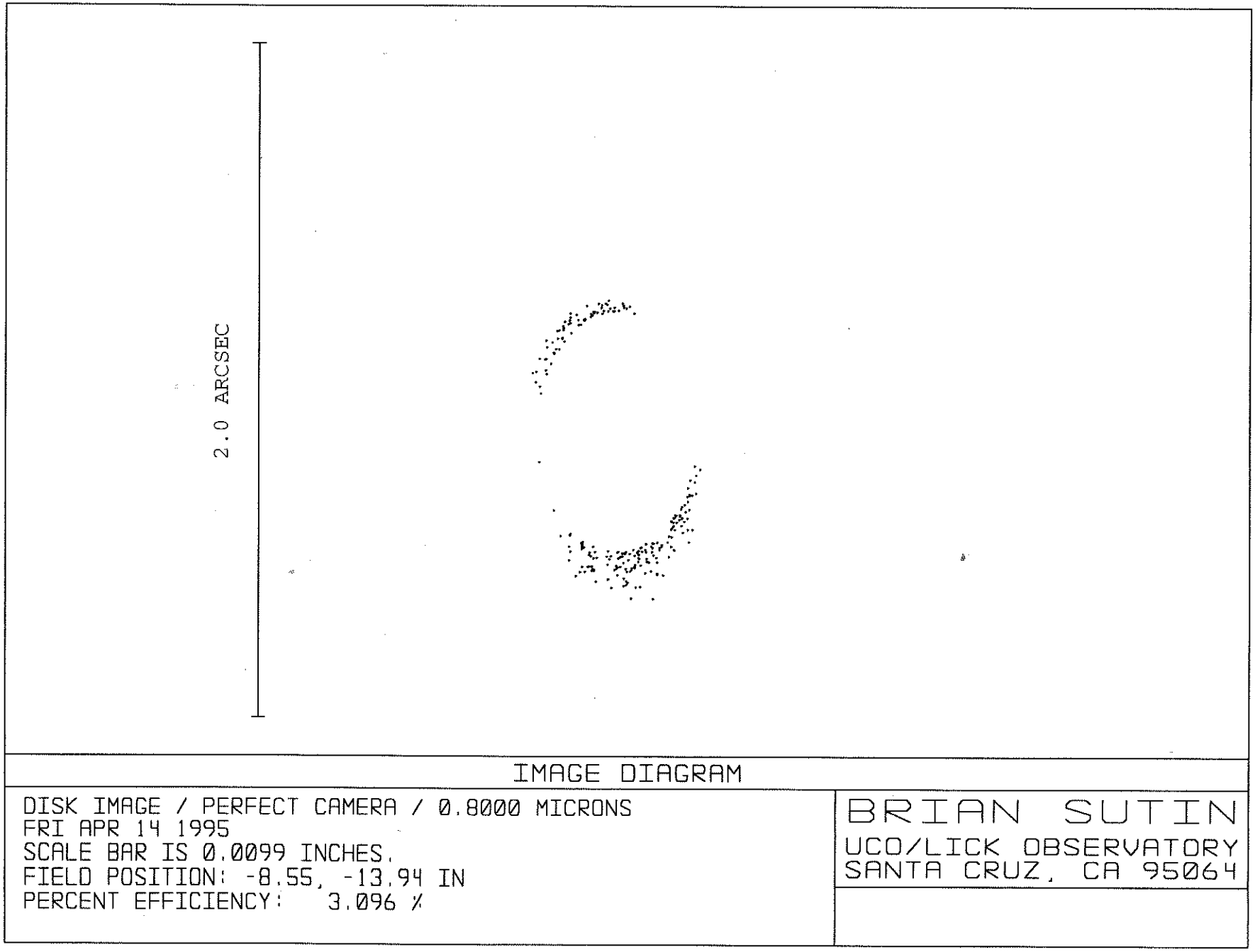
2.0 ARCSEC
IMAGE DIAGRAM
DISK IMAGE / PERFECT CAMERA / 0.8000 MICRONS
FRI APR 14 1995
SCALE BAR IS 0.0099 INCHES.
FIELD POSITION: -8.55, -13.94 IN
PERCENT EFFICIENCY: 3.096 %
BRIAN SUTIN
UCO/LICK OBSERVATORY
SANTA CRUZ, CA 95064

Figure 5.9

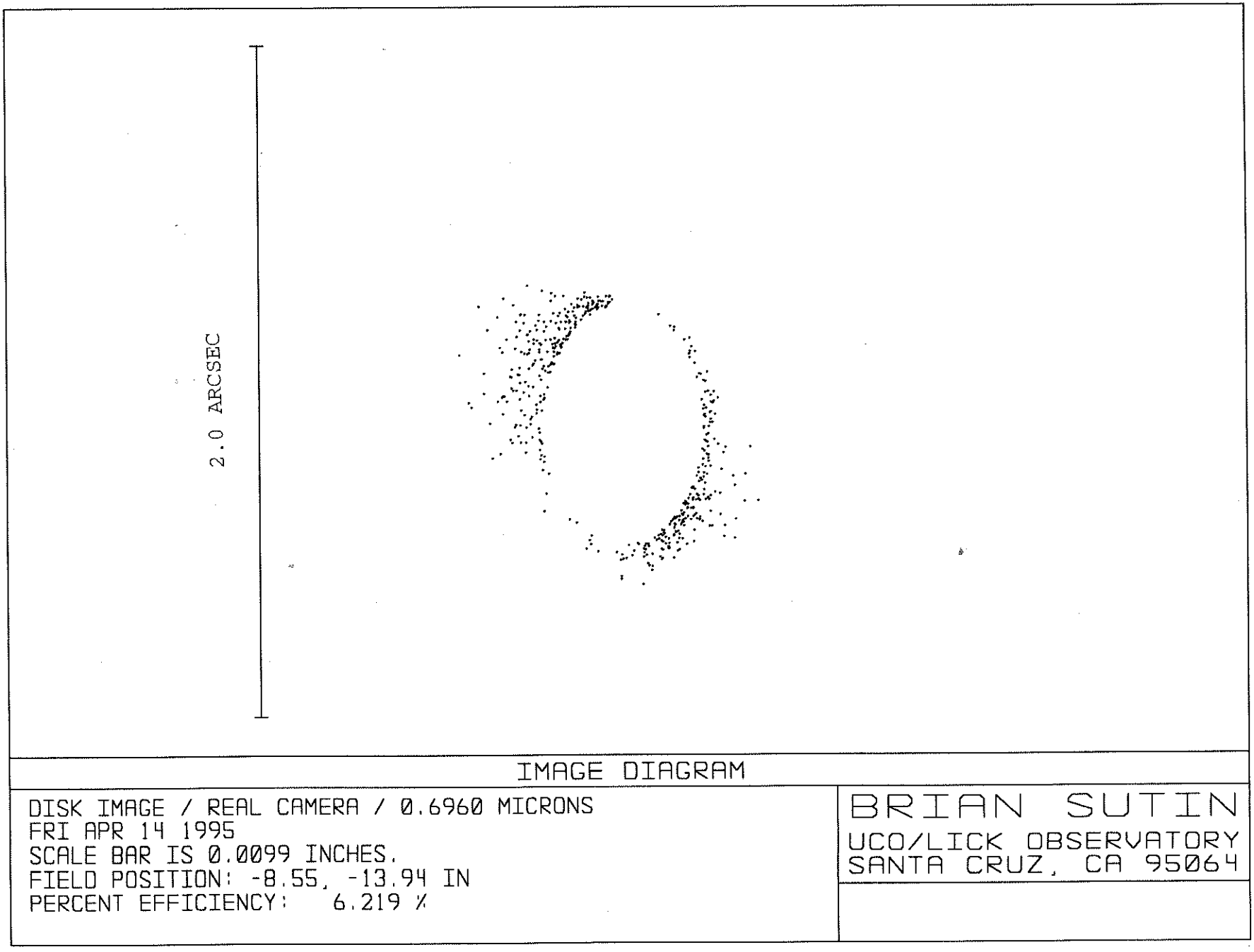
2.0 ARCSEC
IMAGE DIAGRAM
DISK IMAGE / REAL CAMERA / 0.6960 MICRONS
FRI APR 14 1995
SCALE BAR IS 0.0099 INCHES.
FIELD POSITION: -8.55, -13.94 IN
PERCENT EFFICIENCY: 6.219 %
BRIAN SUTIN
UCO/LICK OBSERVATORY
SANTA CRUZ, CA 95064

Figure 5.10

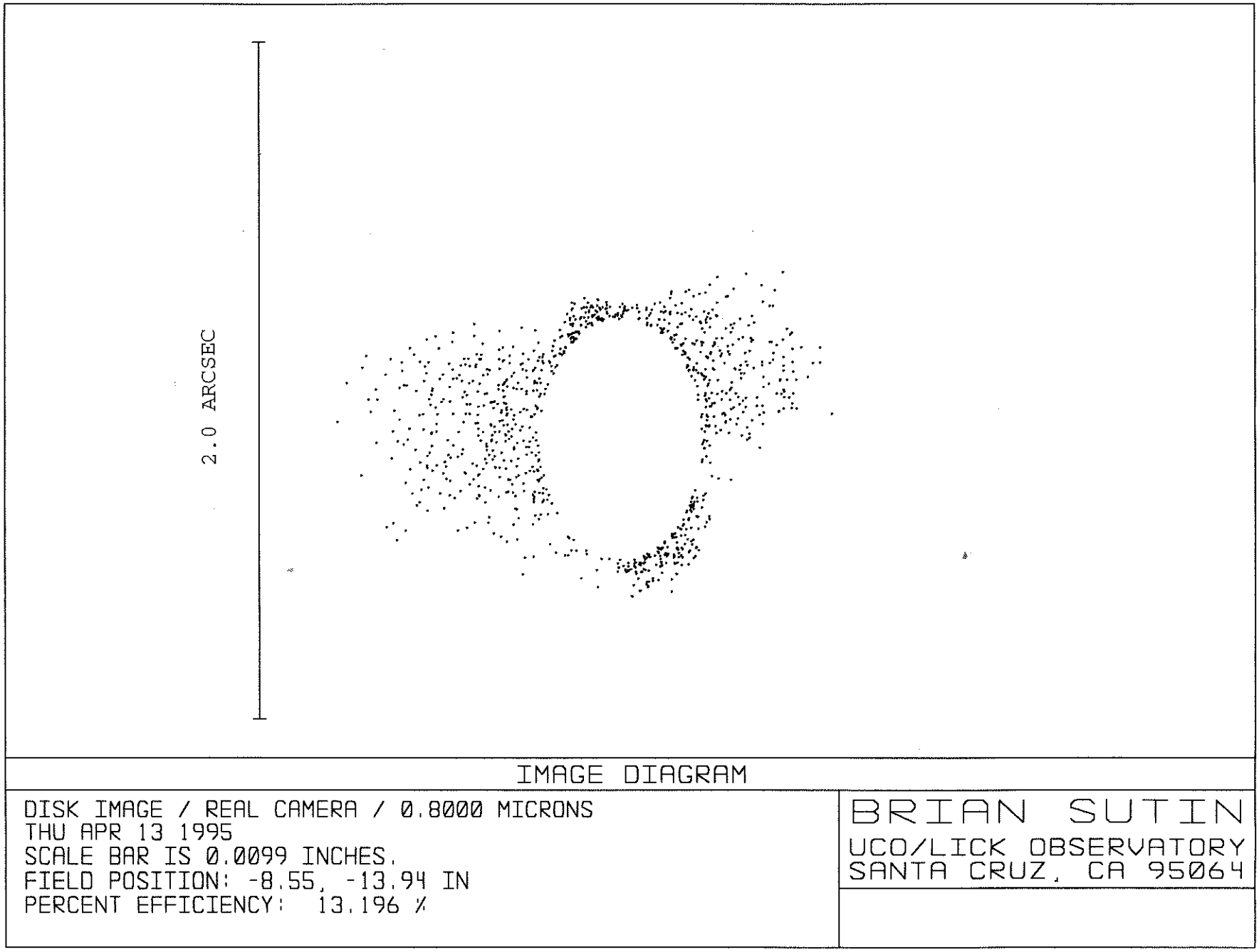
2.0 ARCSEC
IMAGE DIAGRAM
DISK IMAGE / REAL CAMERA / 0.8000 MICRONS
THU APR 13 1995
SCALE BAR IS 0.0099 INCHES.
FIELD POSITION: -8.55, -13.94 IN
PERCENT EFFICIENCY: 13.196 %
BRIAN SUTIN
UCO/LICK OBSERVATORY
SANTA CRUZ, CA 95064

Figure 5.11

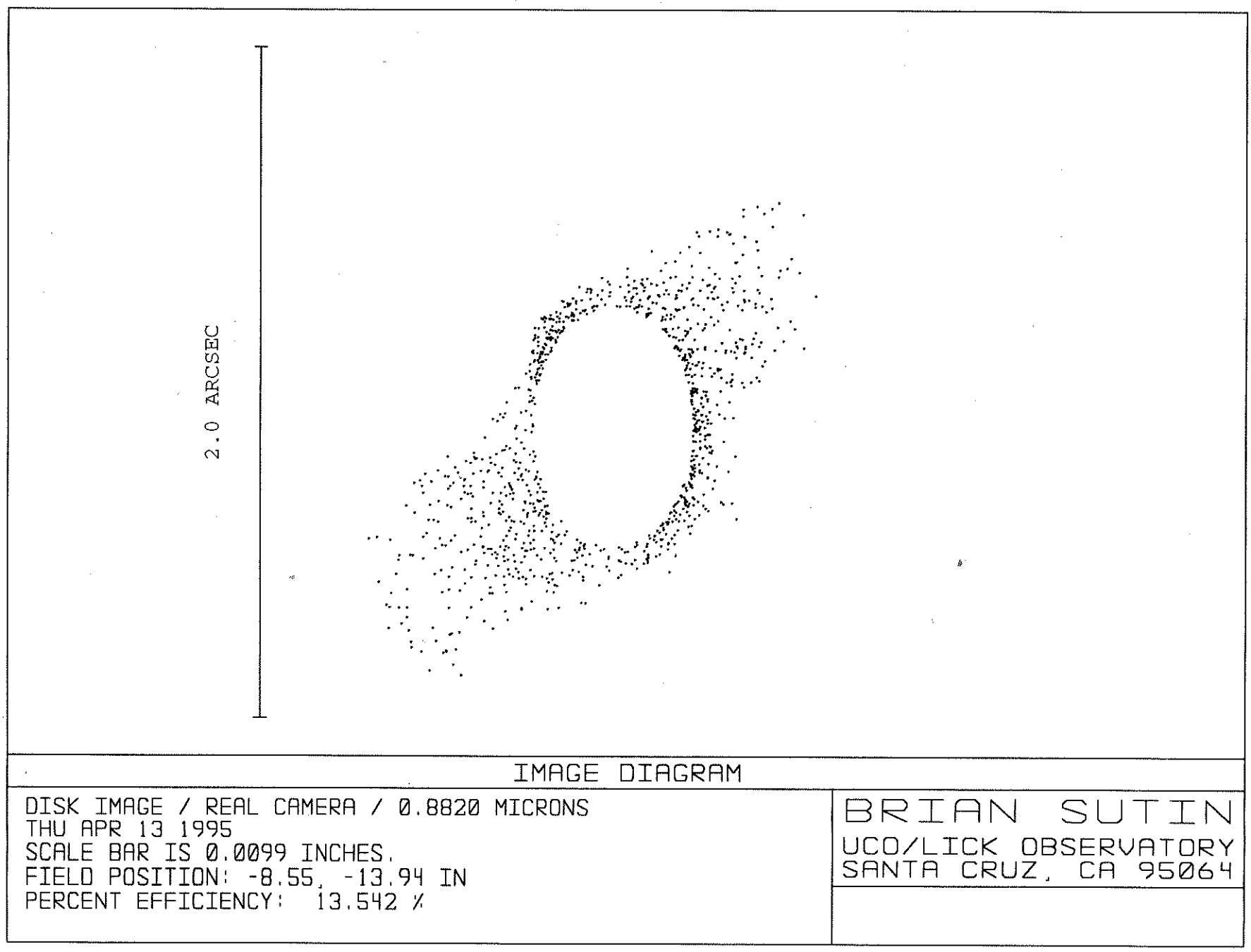
2.0 ARCSEC
IMAGE DIAGRAM
DISK IMAGE / REAL CAMERA / 0.8820 MICRONS
THU APR 13 1995
SCALE BAR IS 0.0099 INCHES.
FIELD POSITION: -8.55, -13.94 IN
PERCENT EFFICIENCY: 13.542 %
BRIAN SUTIN
UCO/LICK OBSERVATORY
SANTA CRUZ, CA 95064

Figure 5.12